

Cofactor NAD(P)H Regeneration Inspired by Heterogeneous Pathways

Citation for published version:

Wang, X, Saba, T, Yiu, HHP, Howe, RF, Anderson, JA & Shi, J 2017, 'Cofactor NAD(P)H Regeneration Inspired by Heterogeneous Pathways', *Chem*, vol. 2, no. 5, pp. 621-654.
<https://doi.org/10.1016/j.chempr.2017.04.009>

Digital Object Identifier (DOI):

[10.1016/j.chempr.2017.04.009](https://doi.org/10.1016/j.chempr.2017.04.009)

Link:

[Link to publication record in Heriot-Watt Research Portal](#)

Document Version:

Peer reviewed version

Published In:

Chem

General rights

Copyright for the publications made accessible via Heriot-Watt Research Portal is retained by the author(s) and / or other copyright owners and it is a condition of accessing these publications that users recognise and abide by the legal requirements associated with these rights.

Take down policy

Heriot-Watt University has made every reasonable effort to ensure that the content in Heriot-Watt Research Portal complies with UK legislation. If you believe that the public display of this file breaches copyright please contact open.access@hw.ac.uk providing details, and we will remove access to the work immediately and investigate your claim.

Cofactor NAD(P)H Regeneration Inspired by Heterogeneous Pathways

**Xiaodong Wang,^{1,5,*} Tony Saba,¹ Humphrey H. P. Yiu,² Russell F.
Howe,³ James A. Anderson,¹ and Jiafu Shi^{4,*}**

¹Chemical and Materials Engineering, School of Engineering, University of Aberdeen, Aberdeen AB24 3UE, Scotland, United Kingdom

²Chemical Engineering, School of Engineering & Physical Sciences, Heriot-Watt University, Edinburgh EH14 4AS, Scotland, United Kingdom

³Department of Chemistry, University of Aberdeen, Aberdeen AB24 3UE, Scotland, United Kingdom

⁴School of Environmental Science and Engineering, Tianjin University, Tianjin 300072, China

⁵Lead Contact

*correspondence: x.wang@abdn.ac.uk

*correspondence: shijiafu@tju.edu.cn

SUMMARY

Biocatalysis can empower chemical, pharmaceutical and energy industries, where the use of enzymes facilitates low-energy, sustainable methods of producing high-value chemicals and pharmaceuticals that are otherwise impossibly troublesome or costly to obtain. One of the largest class of enzymes (oxidoreductases, ~25% of the total) capable of promoting bioreduction reactions are vital for the global pharmaceutical and chemical market due to their intrinsic enantioselectivity and specificity. Enzymatic reduction is dependent on a coenzyme/cofactor as hydride source, namely nicotinamide adenine dinucleotide, NADH or its phosphorylated form (NADPH). Given the high cost, stoichiometric usage, and physical instability of NAD(P)H, a suitable method for NAD(P)H regeneration is essential for practical application. This review summarizes the existing methods for NAD(P)H regeneration including enzymatic, chemical, homogeneous catalytic, electrochemical, photochemical and heterogeneous catalytic routes. Particular focus is given to recent progress in developing heterogeneous systems with potential significance in terms of process simplicity, cleanliness and energy/cost saving.

The Bigger Picture

Sustainable chemical processing must consider minimizing the use of the natural resources, toxic materials and energy, and the generation of waste and pollutants, as we face global challenges in energy, resources and the environment. Biocatalysis may contribute to these goals and has been widely used owing to its high activity, selectivity and specificity and low-energy requirement. The practical application of oxidoreductases, responsible for producing critical chemicals and pharmaceuticals, are limited by the dependence on an expensive cofactor that must be regenerated for reuse.

This review introduces cofactor regeneration methods and highlights the use of heterogeneous systems towards enhancing sustainability. Future research should consider the use of hydrogen gas and strategies to improve catalytic efficiency, simplicity, cleanliness and energy/cost saving which will contribute to the UN Sustainable Development Goal of responsible consumption and production for societal benefits.

INTRODUCTION

Biocatalysis has been extensively used in the chemical and pharmaceutical industries for the manufacture of products ranging from speciality¹ to commodity chemicals (ca. 50,000 ton/annum).² Enzymatic specificity and enantioselectivity are critical, notably in the pharmaceutical sector where enzymes are employed in the commercial synthesis of two thirds of chiral products³ that are widely used in new drug syntheses.^{1 4 5} For example, the drug Lipitors (atorvastatin) has recorded a global sale of US\$11.9 billion in 2010 alone,¹ while worldwide prescription drug sales are forecast to reach US\$1,000 billion in 2020,⁶ where approximately 95% of pharmaceutical drugs will be chiral.⁷ Oxidoreductases are one of the largest class of enzymes (~25% of all enzymes) with far ranging industrial and research significance in the reduction of carbonyl groups, acids, C=C double bonds, nitro groups and C–N multiple bonds.^{4 8} However, many of these enzymatic redox reactions require one or more cofactors that are consumed during reaction.⁹ For instance, enzymatic reductions require a cofactor (or coenzyme) as the hydrogen source (hydride donor), notably (reduced) nicotinamide adenine dinucleotide (NADH) and its phosphorylated form (NADPH, see **Figure 1** for their structures) where 80% of known oxidoreductases require the former and 10% require the latter.⁸ In an enzymatic reduction cycle, NAD(P)H serves as a reductant which is oxidized to NAD(P)⁺ (structure given in **Figure 1**), while the substrate is reduced to the target product using the appropriate (production) enzyme, as illustrated in “pathway A” (**Figure 2**). Given the high cost of the NAD(P)H (bulk price per mol: US\$3,000),¹⁰ stoichiometric supply is not economically feasible and an effective system of cofactor regeneration is required to enable practical large-scale application of enzymatic reductions. This is indeed a reason why cofactor-dependent enzymes (*e.g.*, dehydrogenases) are lagging behind ‘simple’ cofactor-independent enzymes (*e.g.*, hydrolases and oxidases) in terms of their implementation in industry.

METHODS OF COFACTOR NAD(P)H REGENERATION

A major difference between the NAD(P)H and NAD(P)⁺ structure is a hydride ion, *i.e.*, H⁻ (H⁺ + 2e⁻). Regeneration of NAD(P)H therefore requires a (catalytic or non-catalytic) transfer of a proton and two electrons (from sacrificial hydride donors) to NAD(P)⁺ (*i.e.*, reduction of NAD(P)⁺). Common sacrificial hydride donors include formate, glucose, phosphite, triethanolamine (TEOA), mercaptoethanol, propanol and molecular H₂ gas, most of which are valuable chemicals but are consumed in regeneration, while some produce further waste byproducts. Typically, the activity of cofactor regeneration can be measured by turnover frequency (*TOF*, the number of moles of NAD(P)H formed per moles of active site per unit time) whereas the efficiency of an in situ regeneration system can be measured by turnover numbers (TN, the number of moles of product formed per mole of cofactor per unit time) and total turnover numbers (TTN, the number of moles of product formed per mole of cofactor during the course of a complete reaction). In general, TTNs greater than 1000 may appear to make a process economically viable.^{4 11} Moreover, selectivity presents another challenge for the regeneration of NAD(P)H (**Figure 2**) as enzymatically inactive byproducts including the isomers 1,6-NAD(P)H and NAD₂ dimer may form irreversibly, leading to a permanent loss of valuable cofactor. Ultimately, the development of NAD(P)H regeneration must consider activity, selectivity, process sustainability (waste and byproduct generation) and more importantly the practical applications, *i.e.*, compatibility with production enzymes. It is noteworthy from the outset that there are systems which suffer from mutual deactivation between the regeneration and enzymatic processes.^{12 13}

In general, methods for cofactor NAD(P)H regeneration can be sub-divided into six categories, namely enzymatic regeneration (*e.g.*, using glucose (GDH) or formate (FDH) dehydrogenases), chemical regeneration (using inorganic salts such as Na₂S₂O₄ and NaBH₄ or dihydropyridine

compounds, *e.g.*, 1,4-dihydropyridines), homogeneous catalytic regeneration (*e.g.*, Rh, Ru and Ir complexes), electrochemical regeneration (including both direct regeneration on the electrode and indirect regeneration using organometallic complexes as hydrogen transfer agents), photochemical regeneration (*e.g.*, copolymers and carbon nitride as photocatalyst) and heterogeneous catalytic regeneration (*e.g.*, using Pt/Al₂O₃). The last of these was recently developed by two of the authors [here](#).¹⁴ Cofactor regeneration has been an appealing topic with several key reviews based on discussion of the first five methods. We can flag critical assessments by Ward and coworkers (recent trends with emphasis on approaches to overcome mutual inhibition),¹² Wu and coworkers (literature survey on the state-of-art research and crucial issues),⁸ Hollman and coworkers (photochemical regeneration,¹⁵ coupling with enzymatic reductions,⁴ nonconventional/non-enzymatic regeneration),¹¹ ¹⁶ Vincent and coworkers (H₂-driven enzymatic regeneration¹⁷ and immobilized enzymes on carbon based materials¹⁸), Liu and Wang (membrane entrapment and solid attachment of cofactors),¹⁹ Liese and coworkers (coupled with ketone reductions),²⁰ Hummel and coworkers (principles and examples of small-scale and industrial applications),²¹ van der Donk and Zhao (developments of technologies between 2000-2003),²² Wichmann and coworkers (lab scale regeneration²³ and regeneration in membrane reactors),²⁴ and Chenault and Whitesides (regeneration for use in organic synthesis).²⁵ In this review, our discussion is directed at potentially promising systems with a “heterogeneous” nature (*i.e.*, using solid-state catalytic materials in liquid media) for clean cofactor NAD(P)H regeneration. This is of great significance because sustainable manufacturing becomes crucial for the pharmaceutical sector, where environmental impact has been highlighted since the 1990s that the process efficiency has been very low and waste to product ratio has been extremely high.²⁶ We first present an overview of NAD(P)H regeneration methods, then discuss in particular the approaches involving heterogeneous

component(s) and finally focus on our own findings obtained using supported metals as heterogeneous catalyst.

Enzymatic Regeneration

Cofactor regeneration using enzymes has been considered as a favorable system and has been the only one applied practically at industrial scale. One of the earliest examples demonstrating enzymatic NAD(P)H preparation from NAD(P)⁺ was published in 1957 when ethanol and ADH were used by Rafter and Colowick.²⁷ Enzymatic approaches for regeneration offer excellent compatibility with the target bioconversions due to comparable reaction conditions, *i.e.*, low temperature operation in an aqueous media at a near neutral pH (5-9). Moreover, enzymatic regeneration usually associates with a high specific activity, exclusive selectivity towards the active NAD(P)H and low energy consumption. Two common strategies employed are (i) “coupled-enzyme” (**Figure 3A**) which utilizes a second enzyme (*i.e.*, regeneration enzyme) such as GDH with associated sacrificial hydride donor (*e.g.*, glucose) and (ii) “coupled-substrate” (**Figure 3B**) that one enzyme serves both reduction of substrate and cofactor regeneration.²⁸ The most widely used enzymes for cofactor regeneration in commercial processes are GDH and FDH, while phosphite (PDH) and alcohol (ADH) dehydrogenases have been tested at laboratory scale.^{4 29} Other examples include hydrogenase, glucose 6-phosphate dehydrogenase. **Figure 3C** depicts the reaction schemes for these cofactor regeneration systems. Among these enzymes, GDH (*e.g.*, from *Bacillus* species) shows the highest activity (up to 550 U mg⁻¹; U: 1 μmol min⁻¹) and stability, and consequently has become the most widely used. FDH does have a unique feature in generating carbon dioxide (CO₂) as a gaseous byproduct (albeit release to the environment should be minimized) for simplified product separation, but its use is hampered by an associated low activity (~10 U mg⁻¹).

In a “coupled-substrate” system, the single enzyme applied acts as both reducing (production) and oxidizing (cofactor regeneration) catalysts. One classic example is using ADH for the synthesis of the high value drug precursor (S)-2-bromo-2-cyclohexen-1-ol.^{(Calvin, S. J., Mangan, D., Miskelly, I., Moody, T. S. and Stevenson, P. J. (2012) Overcoming Equilibrium Issues with Carbonyl Reductase Enzymes, † *Org. Process Res. Dev.* **16**, 82–86^{need a ref})} In this system, 2-propanol was chosen as the sacrificial hydride donor to form acetone, a volatile byproduct which assisted removal. This approach allows easy scale-up and simplified downstream recovery/reuse of enzyme. However, such systems typically require high concentrations of the sacrificial alcohol to drive the equilibrium towards the desired product. This in turn leads to loss of activity in the main target reaction due to competition amongst substrates and cosubstrates for the same active sites on the enzyme.

Although being the only method industrially employed, cofactor regeneration using enzymes is far from perfect. Firstly, the generation of significant quantities of water-soluble byproducts (*e.g.*, 196 g gluconic acid per mol NADH regenerated by GDH)⁴ requires costly downstream separation and causes enzyme deactivation. Further, addition of base or acid may be needed to maintain the optimal pH for retaining the enzymatic action.⁵ Other disadvantages are linked to the high cost, instability of enzymes and complexity of product purification. As a result, research and development for cofactor regeneration are driven towards systems that show high stability, sustainability and enhanced downstream product separation/purification.

Chemical Regeneration

Chemical regeneration involves use of the high redox potential of salts or dihydropyridine compounds to reduce NAD(P)^+ to NAD(P)H , which can be considered as a non-catalytic process. Common reducing agents used include sodium dithionite ($\text{Na}_2\text{S}_2\text{O}_4$), sodium borohydride (NaBH_4), and 1,4-dihydropyridines. For instances, Jones *et al.*³⁰ in 1972

reported the possibility of utilizing $\text{Na}_2\text{S}_2\text{O}_4$ at a preparative scale and later in 1976 reported the use of a group of reducing 1,4-dihydropyridines with different functional groups (such as $-\text{CONH}_2$, $-\text{CO}_2\text{C}_2\text{H}_5$, $-\text{COOH}$, $-\text{CON}(\text{CH}_3)_2$, etc.).³¹ Since the corresponding turnover numbers of this process are very low ($\text{TTN} < 100$) and high concentration of reductant salts can cause enzyme deactivation,^{8 32} this method has only interest from a historical perspective. It is noteworthy that these methods based on non-catalytic chemical reactions (reducing potentials) have not been widely used due to intrinsic issues that include large amount of feed required and wastes generated, whose high concentration deactivates [the](#) production enzymes.

Homogeneous Catalytic Regeneration

Cofactor regeneration using homogeneous catalysis has been reported since the 1980s using organometallic complexes as the catalysts with molecular hydrogen as the hydride source^{33 34 35}. The most commonly employed catalysts for this purpose are complexes of transition metals such as Rh, Ru, Ir and Pt, which are known to catalyze reductions. Among them, the versatile cationic pentamethylcyclopentadienyl (Cp^*) rhodium bipyridine complex $[\text{Cp}^*\text{Rh}(\text{bpy})\text{Cl}]^+$ has been most widely used due to its flexible (electro)chemical regeneration and regiospecific performance.³⁶ A similar approach is the combination of a Pt carbonyl cluster with the dye safranine in a two-phase system.³⁷ There are also examples of using these organometallic complexes supported on electrodes for electrochemical regeneration of cofactor (which will be discussed later). When compared with enzymes, these organometallic complexes usually exhibit a lower catalytic activity ($k_{\text{cat}} = 0.5\text{--}10$ vs. $\sim 100 \text{ min}^{-1}$ for enzymes), lowering their competitiveness against the enzymatic counterpart.^{12 13} Another major obstacle for large scale application of cofactor regeneration using homogeneous organometallic catalysts lies in their strong interaction with peptide components in enzymes, causing mutual deactivation.¹³ However, progress made in water-soluble organometallic catalysis has shown *TOFs* up to

$\sim 1000\text{ h}^{-1}$ (over $\text{Cp}^*\text{Rh}(5,5'\text{-CH}_2\text{OH-bpy})\text{Cl}]^+$)³⁶ and 2000 h^{-1} (over $[(\eta^5\text{-C}_5\text{Me}_5)\text{Rh}(1,10\text{-phenanthroline})\text{Cl}]^+$ with demonstrated enzymatic compatibility),³⁸ respectively; but both were operated at 60°C and still require an organic hydride donor (*i.e.*, formate). Toxic organometallic complexes and the necessary energy-intensive separation stages are disadvantages.

Electrochemical Regeneration

The electrochemical methods for NAD(P)H regeneration have long been acknowledged as attractive due to the low cost of electricity and the easy control of electrode potentials.²¹

Regeneration could be achieved ~~in~~ from direct, indirect or indirect enzyme-coupled recycling systems (**Figure 4**). For direct regeneration (**Figure 4A**), NAD(P)⁺ is reduced on the electrode surface *via* a 2-step reaction mechanism. In the first step, the oxidized species reacts with one electron to give a radical form, which, in turn, is reduced and protonated to give NAD(P)H. However, the radicals obtained in the first step can combine leading to inactive dimers as a side product. ~~+~~ Modification of the electrode surface by deposition of metal particles was used to increase the protonation rate of the NAD(P) radicals, but again not much of the active NAD(P)H remained after a few regenerative cycles.³⁹ The problems of direct electrochemical methods have been overcome by introducing an indirect regeneration pathway (**Figure 4B**) using mediators, which act as electron carriers and can transfer two electrons or one hydride ion in a single step. Unfortunately, it is still very difficult to find a redox mediator that can regenerate NAD(P)H effectively with high *TOFs*/TNs. Hence, attempts have been made to recycle the cofactors indirectly by coupling the electrochemical redox system with an enzymatic process (**Figure 4C**). Although the mediators and enzymes used are still soluble forming a homogeneous system, the electrodes and associated catalytic materials are solid and as such can be considered as a heterogenised process. This will be discussed further in a following section.

Photochemical Regeneration

Photocatalytic regeneration borrows the concept of photosynthesis in nature that utilizes light-harvesting systems (LHSs) for generating electrons and electron transport chains (ETCs) for migrating electrons to ferredoxin for further NAD(P)H regeneration. This method strongly relies on the development of high-performance photocatalysts. In this regard, a number of organic photosensitizers, inorganic semiconductors, as well as some new materials (*e.g.*, carbon nitride, C₃N₄) have been explored for the regeneration of NAD(P)H. Commonly, organic photosensitizers exhibit better catalytic activity which are 3-100 times better than inorganic semiconductors, of which the synthesis processes are, unfortunately, often complicated and labor-consuming. In contrast, the new materials such as C₃N₄, which are very easy to synthesize show comparable activity to organic photosensitizers, and may be promising photocatalysts for NAD(P)H regeneration. Photochemical regeneration using solid catalysts is a heterogeneous process and will be discussed in a later section.

Heterogeneous Catalytic Regeneration

The origin of NADH regeneration is a reductive reaction from its oxidized form (NAD⁺). A reducing agent and a catalyst are needed to promote such a chemical transformation (NAD⁺ → NADH). Readily available hydrogen gas (preferably from a renewable source) can be a clean source for this purpose with protons as the sole release that can be further consumed in bioconversions, thus achieving 100% atom efficiency (**Figure 5** illustrates enzymatic (FDH) CO₂ reduction as an example, producing formic acid). Such H₂-driven cofactor NADH regeneration exhibits clear advantages in terms of process simplicity and cleanliness. Heterogeneous catalysts (*e.g.*, supported metals) are well-established in activating hydrogen (over *e.g.*, Pt, Pd, Rh, Ru, Ni, Au and Ag) and promoting reduction reactions with the added benefit of facile downstream separation. It would appear to be a straightforward process yet to

the best of our knowledge, only we have reported selective reduction of NAD⁺ using supported metals and hydrogen.¹⁴ This review focuses on this method with detailed discussion in the penultimate section.

Table 1 compares all the critical components involved in the six categories of methods for the regeneration of NAD(P)H cofactor. It is clear that regeneration using heterogeneous catalysts fulfil all four criteria (*e.g.*, avoiding the use of water-soluble catalyst, organic sacrificial hydride donor, mediator and minimizing byproduct generation), showing great potential for cleaner processes. In the following sections, heterogeneous systems for NAD(P)H regeneration that include (i) heterogenized biocatalysis (enzyme immobilization), (ii) heterogenized homogeneous catalysis (organometallic complex immobilization), (iii) electrocatalysis, (iv) photocatalysis (using solid catalysts) and (v) heterogeneous catalysis (supported metal catalysts) will be summarized and discussed in detail.

HETEROGENIZED BIOCATALYSIS

For large-scale industrial operations, enzymatic regeneration of cofactor NAD(P)H is still preferred due to its high activity and use of mild operating conditions.⁴⁰ Several enzymes are capable of regenerating NAD(P)H, in the presence of sacrificial substrates; **Table 2** summarizes the characteristics of these enzymatic regeneration systems. However, similar to the synthetic homogeneous catalyst counterparts, soluble enzymes are difficult to recycle and reuse. Moreover, some of these systems also generate soluble byproducts (see **Table 2**) which require laborious downstream separation. In order to enhance the sustainability, as well as reduce operational cost of these enzymatic regeneration systems, heterogenization of enzymes by immobilization has been reported for use in cofactor regenerations.

There are many immobilization methods for enzymes available in the literature and immobilized enzymes are widely used in industry for facilitating catalyst recycle and reuse.⁴¹

In general, these methods can be classified into a few categories including; crosslinking, entrapment, physical adsorption on a carrier and chemical binding to a carrier (see **Figure 6**). Depending on the systems of interest, each method has its own positive and negative features. Numerous reviews with details of enzyme immobilization can be found in the literature.^{42 43 44} It is commonly accepted that enzyme immobilization enhances recycle and reuse of enzymes, which can be expensive. It also simplifies downstream separation or purification of products. In some cases, immobilized enzymes show higher stability and longer life time than free enzymes.⁴⁵ However, lower activity is generally observed with immobilized enzymes when compared with their free counterparts due to mass transfer constraints. With the benefits on both economy and sustainability, immobilized enzymes are still worth consideration as heterogeneous systems for cofactor regeneration. Indeed, use of immobilized enzymes for cofactor regeneration was reported as early as 1975 when Wykes *et al.* demonstrated a NADH regeneration system using immobilized ADH and lactate dehydrogenases (LDH) on cellulose.⁴⁶ The following are several key examples of cofactor regeneration systems using immobilized enzymes.

Immobilized FDH

FDH converts formate (or formic acid) to CO₂ in the presence of a cofactor NAD⁺.⁴⁷ It possesses one distinctive feature; CO₂ gas is the only byproducts and does not require separation so downstream product purification becomes simpler. However, CO₂ is a greenhouse gas whose release should be always treated cautiously. Immobilization of FDH for cofactor regeneration has been demonstrated.^{48 49} For example, NADH regeneration using entrapped FDH in a poly(vinyl alcohol) (PVA) hydrogel has been studied by measuring the CO₂ release kinetics.⁴⁸ FDH has also been immobilized on commercial polymer beads (Immobead 150) for NADH regeneration. However, the activity was found to drop to less than

70% after 10 cycles.⁴⁹ Immobilized FDH has also been shown active as an *in situ* cofactor regeneration system. Demir *et al.* reported a system for the transformation of hydroxyacetone to a chiral (*S*)-1,2-propanediol with *in situ* NADH regeneration using FDH immobilized on magnetic nanoparticles (Fe₂O₃). However, this system requires a His(6)-tagged FDH, which was not commercially available and had to be extracted from bacteria, for binding onto the amine-functionalized Fe₂O₃.⁵⁰ A continuous feed system for L-lactate synthesis from pyruvate with *in situ* NADH regeneration using FDH supported on alkylated chitosan layers has also been reported. The regeneration system was shown to be active after 2 weeks but with only 50% of the initial activity retained. Nonetheless, this “continuous” regeneration for cofactor demonstrated engineering advances in coupled system for the production of chiral products.⁵¹

Immobilized hydrogenase

Cofactor regeneration using immobilized hydrogenases have also been demonstrated recently.^{52 53} The merit of using hydrogenases for regeneration is associated with the cleanliness; using gaseous H₂ as the sacrificial substrate with H⁺ being the sole byproduct.⁵⁴ However, unlike FDH, hydrogenases for cofactor regeneration are not widely available commercially with solubility and stability being the main concerns. Immobilization of hydrogenases does improve their stability and enhance recycling. For example, soluble hydrogenase from *R. eutropha* has been immobilized on porous glass with a 15-fold improvement in enzyme half-life from 10 h to >150 h. However, the immobilization yield was only 23% and showed significant loss of enzyme.⁴⁷ The stability of immobilized soluble hydrogenase on a polymer methoxy-poly(ethylene) glycol (mPEG) has also been studied in organic solvents and ionic liquids.⁵⁵ Although it showed a 5-fold improvement in half-life from 0.1 to 0.5 h and retained 91% activity of the free enzyme, further improvement are still necessary in order to promote immobilized hydrogenases for use in large-scale synthesis.

Immobilized ADH and GLDH

The other two enzymes commonly used for NADH regeneration are ADH and glutamate dehydrogenase (GLDH). In both cases, sacrificial substrates (alcohol and L-glutamate respectively) are required but, unlike regeneration using FDH or hydrogenase, the byproducts (aldehyde and 2-ketoglutarate) may require further downstream separations. For example, immobilized GLDH on polystyrene particles has been used for NADH regeneration in a 3-step conversion of CO₂ to methanol.⁵⁶ The three enzymes for CO₂ conversion were coimmobilized on one support in order to simplify downstream separation but a stoichiometric supply of L-glutamate (3 mol for 1 mol of methanol produced) is required, leading to a significant amount of waste product. On the other hand, use of immobilized ADH for NADH regeneration may present an advantage over other systems. Immobilized ADH has been used as a “bi-functional” catalyst for both conversion of aldehyde to chiral alcohol products and cofactor regeneration in a “coupled-substrate” system.⁵⁷ Nagayama *et al.* demonstrated the enantioselective reduction of prochiral 4-methyl-2-pentanone to chiral (*R*)-4-methyl-2-pentanol using immobilized ADH (physically adsorbed on glass beads), which was also used for cofactor regeneration using propanol as the sacrificial substrate. For clean use of immobilized enzyme for cofactor regeneration, ADH and GLDH may not be the best candidate.

Whole cell immobilization

When the enzyme required lacks stability, immobilization of the whole cell without enzyme extraction/purification may be an option. Many enzymes are extracted from microbial cells such as bacteria and then purified but these two steps can cause significant losses as well as denature of the enzymes. As a result, whole cell immobilization may be carried out to facilitate recovery, recycling and reuse. Whole cell immobilization has also been used in cofactor regeneration. For instance, yeast cells have been immobilized on alginate fibers for NADH

regeneration.⁵⁸ Although enzyme loss can be avoided, whole cell immobilization can cause side reactions because more than one type of enzymes are likely to be found in each cell, reducing the selectivity of the system. For chiral drug and fine chemical synthesis, whole cell immobilization may not be appropriate.

Immobilized cofactor

The high cost of cofactor is the driving force for regeneration. This also leads scientists/engineers to consider immobilizing cofactors for efficient recovery and reuse. For example, Chen *et al.* have recently demonstrated immobilizing NADH cofactor on chitosan coated magnetic nanoparticles with EDC (1-ethyl-3-(3-dimethylaminopropyl) carbodiimide hydrochloride) and NHS (N-hydroxysuccinimide) (full name?) linkers.⁵⁹ As such, the cofactor can be recovered using an external magnet. A similar approach for cofactor immobilization has also been introduced by Li *et al.* using non-magnetic nanoparticles.⁶⁰ Over 60% of the activity had been retained after 6 cycles. However, similar to enzyme immobilization, lower activity is likely to be observed from cofactor immobilization when compared with free cofactors due to slower mass transfer. Such loss needs to be compensated by recycling and reuse of cofactor.

HETEROGENIZED HOMOGENEOUS CATALYSIS

Similar to enzymes, synthetic homogeneous catalysts can be heterogenized via immobilization on a carrier. So far there has only been one example of using immobilized organometallic complex on a support to form a heterogeneous and recyclable regeneration catalyst. Hollmann and coworkers⁶¹ have immobilized Rh(III)-TsDPEN (an analogue of $[\text{Cp}^*\text{Rh}(\text{bpy})(\text{H}_2\text{O})]^{2+}$) onto surface functionalized poly(ethylene) sinter chips. The activity of this catalyst was approximately one order of magnitude lower than that of the soluble $[\text{Cp}^*\text{Rh}(\text{bpy})(\text{H}_2\text{O})]^{2+}$ (*TOF* of 2.5 h^{-1} vs. 36 h^{-1}), which was attributed to severe diffusion limitations, similar to observation from immobilized enzymes. The solid catalyst could be reused for at least 10 times

but suffered from an activity decrease (by ~50%). One advance from this system is that interaction between the organometallic catalyst and enzyme can be reduced, minimizing the extent of mutual deactivation. Although there are still several issues (*e.g.*, low activity, deactivation) to be addressed with further research, this approach is a conceptually interesting move from soluble to insoluble organometallic complexes, which may improve catalyst cost and incompatibility of Rh with some biocatalysts.

ELECTROCATALYSIS

Cofactor regeneration using electrochemical methods can also be viewed as a heterogeneous process. Bare electrodes made from mercury⁶² and carbon materials⁶³ were used as first attempts to understand the kinetics and mechanisms of NAD(P)H regeneration. It was demonstrated by applying high cathodic potentials (*ca.* -1.6-V) that the formed radicals could be partially reduced to NAD(P)H, preventing the formation of inactive dimers (**Figure 7**). However, protonation of the radicals is not selective resulting in the formation of inactive 1,6-NAD(P)H side products.

Representative studies in direct electrochemical regeneration of cofactor NAD(P)H have been summarized in **Table 3**.^{64 65 66 67 68 69 70} Baik *et al.*⁶⁴ studied the reduction of NAD⁺ using both bare and cholesterol-modified Au amalgam electrodes. Regeneration on the unmodified electrode gave only 10% of enzymatically active NADH. However, when the electrode was modified with a cholesterol membrane, the latter acted as an inhibitor for the NAD radical dimerization leading to a 75% yield of active NADH. After a reaction time of 21 h, a TNN of 1400 was estimated. Conductive vanadia-silica xerogels were used by Park *et al.*⁶⁵ to increase the conductivity of the reaction medium. Regeneration of NADH was coupled to the production of L-glutamate catalyzed by GLDH, and the reaction was complete in 3 h with a TTN of 3300 with respect to NAD⁺.

It has been proven by Omanovic *et al.*^{66 67 68 69 70} that the yield of active NADH regenerated strongly depends on the electrode material. A series of bare Au, bare Cu and Pt-modified Au (Pt-Au) electrodes were used first.⁶⁶ At high cathodic potentials (-1.1V *vs.* Saturated Calomel Electrode (SCE)), the yield of active NADH obtained was 29.6% on Au, 52% on Cu and 63% on Pt-Au. This was explained by the fact that the hydrogen produced in the reduction reaction, enhanced the mass-transport flux of NAD⁺ towards the cathode surface. A further increase in the cathodic potential using a glassy carbon electrode (-2.3V *vs.* Mercurous Sulfate Electrode (MSE)) resulted in a higher yield of NADH (98%).⁶⁷ The same group has been able to further expand their studies in the usage of bare electrodes for the regeneration of NAD(P)H. This time a glassy carbon electrode was modified with electrochemically deposited Pt and nickel nanoparticles.⁶⁸ The role of Ni and Pt particles was to speed up the protonation process by providing active adsorbed hydrogen (Ni-H_{ads} and Pt-H_{ads}). Small average particle sizes (79 nm for Pt and 83 nm for Ni) and narrow particle size distributions were responsible for the enhanced performance of the electrode. In addition, results showed a 100% recovery of active NADH at more positive potentials (-1.5V *vs.* MSE).

Product purity and NADH regeneration kinetics have been recently proven to depend not only on electrode potential but also on the electrode material itself, both controlling the H_{ads} surface coverage and the metal-hydrogen (M-H_{ads}) bond strength. It was further shown that a bare Ti electrode exhibited the highest yield of enzymatically active NADH (96%) at an even lower cathodic potential (-0.8V *vs.* Normal Hydrogen Electrode (NHE)) compared to unmodified Ni, Co and Cd cathodes.⁶⁹ In order to further investigate the effect of surface-modified electrodes, an Ir/Ru-oxide coating was prepared on a Ti plate.⁷⁰ Although Ir and Ru are known to offer a high M-H_{ads} bond strength, it was found that at a potential of -1.7V *vs.* MSE only 88% of NADH were active. This was explained by the hydrogen evolution reactions (Eqs. 1 and 2) that compete with the NAD-radical protonation, hence decreasing the selectivity to NADH.



Problems associated with the direct electrochemical regeneration of NAD(P)H can be overcome by the application of redox catalysts or mediators.^{71 39} In order to be efficient, mediators must fulfil the following criteria:⁷²

- Ability to transfer two electrons or one hydride ion in only one step.
- Activation at potentials more positive than -0.9-V to prevent direct NAD(P)⁺ reduction.
- High selectivity towards the enzymatically active NAD(P)H.
- Avoidance of electron transfer to the enzymatic substrate.

Representative work in indirect electrochemical regeneration of cofactor NAD(P)H has been given in **Table 4**.^{73 74 75 76 77 78} Steckhan *et al.* have worked thoroughly on the elaboration of active organometallic redox mediators (*e.g.*, Rh complex). A typical Rh organometallic mediator accepts two electrons at the surface of the electrode and by inserting a proton into its coordination sphere. The resulting hydride ion is then transferrable to the cofactor. One of the first substances to meet the above requirements was (2,2'-bipyridyl)Rh complex.⁷³ It is worth pointing out that these “redox” mediators are similar in structure/nature to those synthetic homogeneous catalysts used for cofactor regenerations. This mediator was able to reduce cyclohexanone to cyclohexanol with a 26% conversion. However, low TNNs (2.9 with regards to cofactor, and 1.2 with regards to catalyst) were detected as the result of electrode passivation by a layer of [Rh(bpy)₂(H₂O)₂]Cl or [Rh(bpy)₂(OH)₂]Cl deposited on the surface of the cathode. A few years later, a new generation of Rh complexes were developed.⁷⁴ It was possible by using the Cp(Me)₅ ligand to improve the performance of the mediator and obtain 70% conversion of pyruvate to D-lactate with an enantiomeric excess (ee) of 93.5%, and turnover numbers of 7 for the cofactor and 14 for the mediator.⁷⁴

Oxidized NAD(P)^+ cofactors were also reduced to NADH and NADPH using (pentamethylcyclopentadienyl-2,2'-bipyridine aqua) Rh mediator in an electrochemical cell constituted of packed bed graphite particles as a working electrode.⁷⁵ It was found that the TN for the redox catalyst was affected by the size of the carbon particles. Using NAD^+ as cofactor, a TTN of 400 was achieved with 80-200 μm carbon particles and which was clearly better than 40 obtained with 200-400 μm particles. 99% of the produced NADH was enzymatically active. On the other hand, a TTN value of 200 was achieved for the 80-200 μm particles in the reduction of NADP^+ .

$\text{Cp}^*[\text{Rh}(5,5'\text{-methyl-2,2'-bipyridine})]$ (**1**) and $\text{Cp}^*[\text{Rh}(4,4'\text{-methoxy-2,2'-bipyridine})]$ (**2**) complexes were able to reduce NADP^+ three times faster than the previous established mediators.⁷⁶ A *TOF* of 97 h^{-1} and a reduction rate of 116 mM d^{-1} were achieved using catalyst (**1**), whereas a *TOF* of 113 h^{-1} and a reduction rate of 136 mM d^{-1} were observed using catalyst (**2**).

Unfortunately, coupling the indirect electrochemical regenerative systems by Rh complexes to an enzymatic synthesis reaction can result in the deactivation of the enzyme,⁷⁴ a similar observation to “mutual deactivation” in synthetic homogeneous regeneration systems. A membrane electrochemical reactor (MER) was applied to overcome this limitation. Lutz *et al.*⁷⁷ successfully developed a stable electro-enzymatic process by means of an enzyme-catalyst separation. For this purpose, a polymeric mediator was synthesized by polycondensation of 2,2'-bipyridine-4,4'-di-aldehyde and α, ω -functionalised amino polyethylene glycol. This prevents direct contact between mediator and enzyme. A 90% substrate conversion was observed. Nevertheless, this system allowed the recovery of 86% of the mediator, resulting in a TTN of 214. Minter *et al.*⁷⁸ have recently made a useful contribution to the immobilization of redox catalysts in the regeneration of NADH. In this work, immobilization of the pyridine-

Rh complex took place on multi-walled carbon nanotubes (MWCNs) by means of π - π stacking effect, in which an aromatic moiety is attached to the catalyst allowing the latter to strongly adsorb on the electrode surface. An exceptional average *TOF* of 3.6 s⁻¹ was observed over 10 cycles using 2 mM of NAD⁺.

Direct and indirect electrochemical regeneration of NAD(P)H have not proven to give sufficient efficiency in cofactor regeneration. Moreover, as it was difficult to design a redox mediator/catalyst that meet all criteria mentioned previously, attempts have been made to couple the indirect electrochemical regenerative system with an enzymatic process.³⁹ Many examples can be found in literature where various mediators such as organic methyl viologen,⁷⁹ and flavins⁸⁰ were assisted by enzymes such as reductase,⁸¹ lipoamide dehydrogenase (LipDH),⁷⁹ diaphorase, and hydrogenase.⁸²

Representative studies in enzyme-coupled indirect electrochemical regeneration of cofactor NAD(P)H have been summarized in **Table 5**.^{79 83 84 85 86 87 88} Using cyclic dithiols as mediators along with LipDH as enzyme, Whitesides *et al.*⁸³ were able to obtain TTNs of 920 for NAD⁺ and 13 for the enzyme, after the reaction was completed in 3.5 days. However, only 5% of the NADH remained active, indicating a low selectivity. Introducing other types of mediators, higher residual activities were detected. Coupling methyl viologen with LipDH resulted in 51% active NADH and 65% active LipDH. Moreover, 68% residual activity for the cofactor and 80% for the enzyme were observed in the reduction of NADP⁺ by means of methyl viologen and ferredoxin-NADP-reductase (FDR).⁷⁹

In an attempt to produce (*R*)-mandelate from benzoylformate in the presence of benzoylformate reductase (BFR), methyl viologen mediator was used alongside diaphorase enzyme.⁸⁴ Although the reaction exhibited 80% conversion in 30 hours, methyl viologen

contributed to the loss of 50% of BFR activity after 6 days. Instead, the use of flavine adenine dinucleotide (FAD) resulted in a more stable BFR and a 95% reaction conversion in 18 hours.

Regeneration of NADH together with methyl viologen was also reported in the enzymatic reduction of ketones. Since it has been known that enzymes are affected by free methyl viologen in solution, immobilization of mediation components is good practice. Osa *et al.*⁸⁵ employed a poly(acrylic acid) layer-coated graphite felt electrode to immobilize the mediators. They were able to successfully reduce 2-methylcyclohexanone (49.8% conversion, 100% ee, and 91 TTN_{Mediator}) and 3-methylcyclohexanone (51.7% conversion, 93.1% ee and 94 TTN_{Mediator}) to the corresponding alcohols. On the other hand, Tzedakis *et al.*^{86 87} have designed micro-reactors which rely on unmodified Au electrodes, FAD mediator and FDH enzyme, for the continuous regeneration of NADH. The first reactor adopts the principle of laminar-based flow which keeps the reactants close to the electrode and prevents any side reactions. This system was able to retain a 31% NADH yield and a 41% conversion of pyruvate to L-lactate with a TN of 75.6 h⁻¹ for the cofactor.⁸⁶ The second is a filter-press micro-reactor that gave 80 h⁻¹ as NAD⁺ TN.⁸⁷ Immobilized FADs were used in combination with FDH enzyme for the production of L-lactate from pyruvate. This time the FAD mediators were fixed on a carbon cloth as an economical support that provides a high specific surface area. The modified electrode contributed to a 60% substrate conversion after 96 h reaction, compared to a 50% conversion after 120 h with the bare carbon cloth electrode.⁸⁸

Very recently, a new perspective of using carbon materials was introduced where methyl viologen was immobilized on multi-walled carbon nanotubes (MWCNTs).⁸⁹ Glucose oxidase (GO_x) was adopted as a model enzyme for the purpose of NADH regeneration. It was shown that immobilized GO_x accounted for a satisfactory electron transfer rate (e.g.,), which could intensify the potential of this process to be coupled to later organic enzymatic syntheses.

All in all, since it has been challenging to find an efficient and enzyme friendly electron carrier that can overcome the disadvantages of the direct electrochemical regeneration of NAD(P)H, researchers have attempted to use an enzyme along with the mediator to push the TNs up to industrial levels. Unfortunately, by doing so, complications of product recovery and separation have arisen, leaving this regeneration method requiring further studies and investigations.

PHOTOCATALYSIS (USING SOLID PHOTOCATALYSTS)

Nature hints at an alternative way to regenerate cofactor through the photosynthetic process where photo-excited electron transfer regenerates reducing power in the form of NAD(P)H, for a further Calvin cycle.⁹⁰ This process strongly relies on the light-harvesting system, involving two protein complexes (photosystem I and II),⁹¹ and has inspired researchers to explore a diverse range of artificial photosensitizers, including proflavine,⁹² diphenylalanine/porphyrin nanotubes,⁹³ chromophore-bonded graphene nanosheets,^{94 95} cadmium sulfide (CdS),^{96 97} titanium oxide (TiO₂),^{98 99 100} carbon nitride (C₃N₄),^{101 102 103 104} and so on^{105 106 107 108} (Table 6^{106 93 94 95 98 99 97 96 102 103 101}). Due to the limited but efficient species of electron donors (mainly TEOA) and electron mediators (M, mainly pentamethylcyclopentadienyl rhodium bipyridine, [Cp^{*}Rh(bpy)H₂O]²⁺) involved in photocatalytic regeneration of NAD(P)H,^{12 8} we feature here the recent advances in photosensitizers that have exerted superiority in the photocatalytic regeneration of NAD(P)H. Based on chemical composition, the current photosensitizers can be categorized into organic and inorganic types.

Organic photosensitizers

Archiving nature-derived photosensitizers (chlorophyll, proflavine, porphyrins, *etc.*) is a direct way for photo-excitation of electrons and subsequent regeneration of NAD(P)H.^{92 106} Although showing high efficiency, most of these photosensitizers are small molecules, presenting drawbacks of structural instability and difficulty in photosensitizer reusability and

product/photosensitizer separation. Modifying and immobilizing organic photosensitizers onto larger-scale supports is a feasible strategy for their practical applications. Physical entrapment and chemical grafting are two major methods. Park and coworkers¹⁰⁶ are pioneers in applying the physical entrapment to immobilize organic photosensitizer. In brief, they encapsulated porphyrins (light-harvesting pigments) within a porous lignocellulosic support through *in situ* precipitation of porphyrins during lignocellulose coagulation, thus acquiring a light-harvesting synthetic wood (LSW) (**Figure 8A**). During the photocatalytic regeneration of NADH, the porphyrin absorbs photonic energy to create high-energy electrons, which are then transferred to M (the mediator $[\text{Cp}^*\text{Rh}(\text{bpy})\text{H}_2\text{O}]^{2+}$). The activated M further transfers–hydride (H^-) to NAD^+ in a single step, achieving the regeneration of NADH. Meanwhile, a sacrificial electron donor of TEOA reduces the oxidized porphyrin to avoid its degradation. Park *et al.* also evaluated and compared six types of hydrophobic porphyrins with different metal centers and side groups (**Figure 8B**), where the highest *TOF* of $\sim 1.250 \text{ h}^{-1}$ can be achieved with the photosensitizer having mTHPP (give full name first) groups.

Dissimilar from non-specific structural characteristics of lignocellulosic supports, self-assembled hierarchically structured materials often exhibit unexpected functions due to the complex mutual interactions between different moieties. Typically, tubular structures usually exhibit extraordinary performance in electron transfer, which can lower the hole-electron recombination rate. Based on this theory, Park and coworkers⁹³ synthesized diphenylalanine/porphyrin light-harvesting peptide nanotubes through incorporating porphyrin photosensitizer during the self-assembly of diphenylalanine. To further enhance the separation/transfer efficiency of excited electrons from porphyrin to M, Pt nanoparticles were deposited on the surface of the peptide nanotubes. The reduction potential at the cathodic peak current of the Pt-doped peptide nanotubes and M was, respectively, located at 1.2 and 0.7-V (vs. Ag/AgCl), where the energetic relationship between Pt-doped peptide nanotubes and M

was similar to that found in visible-light harvesting system in nature (**Figure 9A and 9B**). In the presence of the Pt-doped peptide nanotubes, the cathodic current of M at its reduction potential was enhanced, confirming that the excited electrons from the nanotubes were transferred to M. The *TOF* of Pt-doped peptide nanotubes was $\sim 1.780 \text{ h}^{-1}$ (**Figure 9C**), suggesting superiority of the tubular structure compared to the lignocellulosic support. The artificial photosensitizer was further applied for photocatalytic synthesis of L-glutamate from α -ketoglutarate, coupled with a cofactor regeneration process. The conversion yield (1.45 mM) of L-glutamate was 2.7 and 48.3 times higher than those acquired from the Pt-doped peptide nanotubes and the sole porphyrin photosensitizer monomers, respectively (**Figure 9D**).

As indicated, physical entrapment offers a simple way to immobilize small organic photosensitizers through manipulating the multiple weak interactions between photosensitizers and the support. Alternatively, chemical grafting provides a more delicate and versatile method for molecule engineering of photosensitizers. It is possible to activate the specific groups of either photosensitizers or supports and then trigger the coupling reaction. Chromophore-bonded graphene nanosheets developed by Baeg and coworkers are one example of the representative immobilized photosensitizers through chemical grafting (**Figure 10A**).^{94 95} This immobilized photosensitizer integrates the superiority of the chromophore in visible-light harvesting and the excellent electron transfer property of graphene, offering high potential in the photocatalytic regeneration of NAD(P)H. For instance, Baeg *et al.* reported a graphene-based visible-light photosensitizer, termed as CCGCMAQSP, in which covalently bonded multianthraquinone substituted porphyrin (MAQSP) was combined with the “chemically converted graphene” (CCG). They also chose two other photosensitizers,¹⁰⁹ $\text{W}_2\text{Fe}_4\text{Ta}_2\text{O}_{17}$ and MAQSP, with lower photocurrent than CCGCMAQSP for comparison. As expected, CCGCMAQSP exhibited the highest *TOF* of 0.375 h^{-1} during NADH regeneration (**Figure 10B**). Through density functional theory (DFT) calculation, the authors further confirmed that

the energy level differences between neighbored segments were aligned for electrons to transfer from MAQSP to the hydrogen reduction site *via* CCG. Similar to Pt-doped peptide nanotubes, CCGCMAQSP was further applied for coupling with enzymatic conversion CO₂ to formic acid by formate dehydrogenase (**Figure 10C**). Although some success has been achieved, Baeg and coworkers still wondered if better photocatalysts can be synthesized (**Figure 10D**). In their subsequent investigation, two chromophoric motifs, isatin and porphyrin (termed as IP), were combined for further grafting onto graphene nanosheets. The resultant CCG-IP exhibited a much higher *TOF* (0.642 h⁻¹, **Figure 10E**) by contrast with CCGCMAQSP. In addition to coupling this photosensitizer with single-enzyme catalysis, Baeg *et al.* also extensively incorporated CCG-IP and CCGCMAQSP into multi-enzyme system for methanol production from CO₂.⁹⁵ A methanol concentration of 11.21 μM was obtained on exposure of the CCG-IP based integrated system to visible light over 60 min (**Figure 10F**). In our opinion, this trial shows the possibility of applying photocatalytic regeneration of NAD(P)H in applications with more complicated reactions.

Although confronting many difficulties, "All-in-One" photocatalytic regeneration systems with integrated organic photosensitizer and M are still actively pursued. Knör and coworkers have performed very exciting work.^{110 111} They synthesized Rh-BipyE-PVab polymer that contains bipyridine-containing poly-(arylene-ethynylene)-alt-poly(arylene-vinylene) copolymer (as photosensitizer) with a redox-active Rh cyclopentadienyl complex (as mediator) (**Figure 11A and 11B**). This Rh-BipyE-PVab polymer was coated on glass beads for photocatalytic regeneration of NADH with formate or TEOA as the electron donor. Due to the integrated property of this photosensitizer, the photon absorption, electron generation and transfer, and the NADH regeneration process all occur in one polymer chain. The amount of regenerated NADH gradually increased with extended reaction time (**Figure 11C**). However, these authors adopted an alternative index to evaluate the regeneration efficiency, which was calculated

based on the surface area of the glass beads. The reaction rate can reach as high as $1.8 \mu\text{mol cm}^{-2} \text{ h}^{-1}$. Although we cannot compare this value with previous results, this Rh-BipyE-PVab polymer shows superiority in many aspects. Specifically, in contrast to existing systems with molecule-sized Rh complexes, the Rh-BipyE-PVab polymer works as both an immobilizing support and photosensitizer, which can avoid the loss of mediator, and minimize the contact of catalyst with NADH-binding site of enzymes when applied in coupled photo-enzymatic catalytic systems.

Collectively, organic photosensitizers have exerted high efficiency in photocatalytic regeneration of NAD(P)H (**Table 6**), while their molecule-scale nature seriously restricts further applications without proper immobilization. In this context, some researchers have already transferred their attention to inorganic photosensitizers with a particular structure, which is introduced in the following section.

Inorganic photosensitizer

As a typical inorganic photosensitizer, TiO_2 is the first choice for light-driven photocatalytic regeneration of NADH.^{112 113} However, pristine TiO_2 has a band gap of $\sim 3.2 \text{ eV}$, which means that electrons can only be excited by ultraviolet light (UV, accounting for only 4% of the sun's energy). More importantly, high-energy UV luminescence usually leads to rapidly increases in temperature that seriously harm biomolecules. Therefore, NAD(P)H regeneration systems enabled by pristine TiO_2 are inappropriate for coupling with enzyme catalysis. Many efforts have been devoted to narrowing of the band gap through modifying TiO_2 . Jiang and coworkers have contributed significantly in this area.^{98 99 100} They explore a general strategy of doping non-metal elements (including carbon, boron, nitrogen, phosphorus, *etc.*) to examine whether the doped element has this function. They initially synthesized carbon-doped TiO_2 through sol-gel process using titanium oxide with ethanol and acetic acid as carbon sources.⁹⁸ The carbon

doping indeed narrows the band gap of TiO_2 , causing a red shift of the absorption edge, and enhances the absorption of visible light. Under visible light irradiation, the carbon-doped TiO_2 exhibits high activity and selectivity towards enzymatic active NADH in the presence of M and the electron donor. Jiang *et al.* also investigated the influence of several factors, including electron donor species, pH, M concentrations, etc., on the regeneration efficiency of NADH. Phosphorus and nitrogen can also be doped in TiO_2 ,^{99 100} and function similarly to carbon-doped TiO_2 . Compared with organic photosensitizers as mentioned in the previous section, TiO_2 -based photosensitizers exhibit a much lower *TOF* (0.031 h^{-1}) in NADH regeneration. But, as the first generation of heterogeneous inorganic photosensitizer, modified TiO_2 paves the way of developing other types of inorganic photosensitizers.

Quantum dot nanocrystals (including cadmium sulfide (CdS), zinc sulfide (ZnS), cadmium selenide (CdSe), etc.) are other inorganic photosensitizer after TiO_2 , which are attractive visible-light-harvesting materials due to their suitable band gaps.^{96 105 107} Considering the nanoscale of quantum dot nanocrystals, it is better to dope this highly efficient photosensitizer onto larger-scale support, where silica is preferred. Through simple hydrolysis and the nucleation reactions of an alcoholic silica precursor, Park and coworkers⁹⁷ successfully deposited CdS quantum dots (band gap $\sim 2.4 \text{ eV}$) on the surface of SiO_2 beads by a successive ionic layer adsorption reaction of CdSO_4 and Na_2S . Facilely altering the number of coating cycles can manipulate the amount of CdS nanoparticles formed on the SiO_2 surface. Not only does it act as a support, the SiO_2 can also interact with the metal center (Rh^{2+}) of M. The ionic affinity between the surface $-\text{OH}$ groups of SiO_2 and the metal center of M may boost the energy transfer between SiO_2 and M. Therefore, the photo-excited electrons from CdS could be transferred more efficiently to M. By using CdS-coated SiO_2 for visible-light-driven NADH regeneration, a high *TOF* of 0.278 h^{-1} is obtained, which is nearly ten times higher than that achieved with doped TiO_2 .^{97 98} Furthermore, owing to the heterogeneous feature of this

photosensitizer, no significant decrease in activity is noted during four cycled uses. In terms of CdS-coated SiO₂, it is just speculated, not confirmed, that the interaction between M and SiO₂ support might exist and elevate the electron and energy transfer. This stimulated researchers to fabricate more delicate structures for faster transfer of photo-excited electrons to M. Rational design of "charge steps" in the hetero-structured inorganic photosensitizers to lower the "hole-electron" recombination rate is a simple and popular way to facilitate the charge carrier migration process, by which the photo-excited electrons and holes can be driven to the opposite side of the hetero-junction interface thus inhibiting their recombination rates.¹¹⁴ A typical example of a hetero-junction structure is the combination of two most popular inorganic photosensitizers, *i.e.*, TiO₂ and CdS through coating CdS nanoparticles onto anodized TiO₂ nanotube arrays.⁹⁶ An NADH regeneration experiment enabled by the CdS-coated TiO₂ (CdS-TiO₂) nanotubular film with TEOA as the electron donor has lots of advantages, including easy synthesis, morphology control, rapid charge separation, *etc.* Due to the ~0.2 V more negative position of the conduction band (CB) edge of CdS compared to TiO₂, photo-excited electrons can be rapidly injected from CdS to TiO₂, remarkably suppressing electron–hole recombination. Exploiting the same index to Rh-BipyE-PVab polymer photosensitizer,¹¹⁰ this isotype hetero-junction structured photosensitizer exhibits an extremely high reaction rate (240 μmol cm⁻² h⁻¹). To further support the hypothesis that efficient charge separation in CdS-TiO₂ nanotubular film can enhance the efficiency of NADH photoregeneration, CdS-coated Al₂O₃ (CdS-Al₂O₃) nanotubular film were also prepared. Although comprising similar topological structures, the CdS-Al₂O₃ nanotubular film exhibited much lower NADH regeneration efficiency and turnover frequency, which is ascribed to a higher degree of charge recombination (**Figure 12A and 12B**).

Similar to the Rh-BipyE-PVab polymer developed by Knör and coworkers, an "All-in-One" photocatalytic NAD(P)H regeneration system has been constructed based on CdS. King and

coworkers¹⁰⁷ directly adsorbed ferredoxin NADP⁺-reductase (FNR) onto CdS nanocrystals. Through combination of superfast reduction rate of enzymatic catalysis and direct transfer of photo-excited electrons from CdS to FNR, the resultant FNR@CdS "All-in-One" systems show a remarkable *TOF* of $\sim 1440\text{ h}^{-1}$ (NADPH). Nonetheless, FNR only shows specificity for NADPH regeneration, meanwhile, the FNR@CdS system is not readily recycled due to the small particle size ($< 10\text{ nm}$). This study opens up an interesting way of elevating regeneration efficiency of cofactors through combining two general approaches: biocatalysis and photocatalysis.

Newly emerged photosensitizer: graphitic carbon nitride (g-C₃N₄)

In addition to modified TiO₂ and CdS, few other inorganic or semiconductors have been explored for visible-light-driven photocatalytic regeneration of NADH for a relatively long period. Fortunately, in recent years, a newly emerged photosensitizer, namely graphitic carbon nitride (g-C₃N₄), has elicited excitement in many research communities. Due to its facile synthesis, appealing electronic band structure (band gap, $\sim 2.7\text{ eV}$), high physicochemical stability, and "earth-abundant" nature,¹¹⁵ g-C₃N₄ is viewed as the next generation visible-light photosensitizer. Moreover, as a conjugated polymer, g-C₃N₄ is commonly derived through thermal-induced polymerization of abundant nitrogen-rich precursors. Accordingly, the surface chemistry can be facilely modulated by means of surface engineering at the molecular level, while the structure/morphology can be easily regulated. Antonietti and coworkers^{101 102 103 104} were the first researchers who come up with a strategy of utilizing g-C₃N₄ to photocatalytically regenerate cofactors (**Figure 13A**). In the presence of M and the electron donor, the general process and mechanism of NADH regeneration is similar to that enabled by TiO₂, CdS and other organic photosensitizers. In brief, g-C₃N₄ generates electron-hole pairs under visible light irradiation. The as-generated high-energy electrons from g-C₃N₄ are then transferred and

abstracted by M. Subsequently, M, bearing electrons, selectively regenerates NADH by transferring two electrons to NAD^+ followed by coupling with one proton and region-specific transfer to NAD^+ . The NADH regeneration efficiency can reach nearly 100% with *TOFs* of $0.067\text{--}1.326\text{ h}^{-1}$ that depend on the structures. Most excitingly, g- C_3N_4 can also photocatalytic regenerate NADH in the absence of M. The authors attribute this phenomenon to the following aspects: NAD^+ can be attached to the surface of C_3N_4 through π - π stacking of the heptazine building blocks of the g- C_3N_4 and adenine subunit of the NAD^+ , which leads to the direct transfer of photo-excited electrons to NAD^+ (**Figure 13B and 13C**).¹⁰³ However, due to the absence of M, the number of electrons transferred to NAD^+ is uncontrollable. As a result, the formation of NADH is non-specific, whereas the product usually contains some enzymatically inactive 1,6-NADH. The maximum NADH regeneration efficiency is only $\sim 50\%$ with a *TOF* of lower than 0.665 h^{-1} . However, the importance of this study is to offer a way of simply manipulating interactions between NADH and photosensitizers to acquire M-free NADH regeneration systems. Based on the above achievements, they have synthesized g- C_3N_4 with diverse morphologies, including ~~diatom~~diatom-mimic structure,¹⁰² porous nanospheres,¹⁰³ porous nano-rods,¹⁰¹ frustule-like carbon nitride array,¹⁰⁴ *etc.* The aim of the structure alternation is to enhance the light-harvesting capability, prolong the light retention time, and lower the hole-electron recombination rate. All of the above g- C_3N_4 are coupled with NADH-dependent enzymatic catalysis (including peroxidase, dehydrogenase, *etc.*), verifying the superiority and possibility of C_3N_4 in artificial photosynthesis. Regrettably, no further investigations regarding M-free NADH regeneration systems enabled by g- C_3N_4 have been reported since 2014.

To summarize, the merits of photocatalytic regeneration of NAD(P)H cofactor are reflected in many aspects, of which the most attractive one is the conversion of visible light into chemical energy behaving like nature. Through rationale design and manipulation, light-harvesting

capability can be strengthened, while the hole-electron recombination rate can be suppressed. The newly developed photosensitizers perform better and better in the NAD(P)H regeneration efficiency and in terms of turnover frequency. Recent efforts have been devoted to develop "All-in-One" photosensitizers, which integrate M within photosensitizers. Nonetheless, nearly all of the current photosensitizers still rely on TEOA as the electron donor. The generated oxidized TEOA in the product solution still complicates the final purification process.

HETEROGENEOUS CATALYSIS (SUPPORTED METAL CATALYSTS)

The use of supported metal heterogeneous catalysts for cofactor regeneration was recently reported by some of us.¹⁴ In this section we will describe the work conducted and update with latest results. In order to establish the feasibility of NAD(P)H regeneration catalyzed by supported metals, the process was initially tested by screening a series of commonly used hydrogenation/reduction active catalysts including Al₂O₃ supported (5 wt%) Pt, Rh, Ru, Pd and Ni (6 wt%). It was encouraging to notice (**Figure 14A**) that all of the above catalysts showed some activity towards NADH production from the reduction of NAD⁺ by H₂ (see **Supplemental Information** and reference¹⁴ for experimental details). Since Pt gave a continuous increase in NADH generation, a Pt catalyst of lower loading was investigated *i.e.*, 1 wt%, over both Al₂O₃ and carbon as carriers. A low loading is favorable for NADH regeneration (**Figure 14B**) where Pt/Al₂O₃ outperformed Au/Al₂O₃ in terms of activity and Pt/C in terms of selectivity (the high initial activity of this catalyst is interesting and worthy of further investigation). The concentration of NADH (rather than its [inactive](#) isomer) was also confirmed independently by ¹H NMR analysis (**Figure 14B**), which was in good agreement with the result determined by UV spectrophotometry and demonstrated the heterogeneous catalyst promoted NADH regeneration. This encouraging observation should not be a complete surprise as supported Pt has shown activity in the hydrogenation of compounds with similar

ring structure to NADH (*e.g.*, pyridines),¹¹⁶ and there are studies in the literature relating to photocatalytic¹⁰⁸ and electrocatalytic¹¹⁷ regeneration using Pt nanoparticles as photosensitizer and proton carrier, respectively.

Taking Pt/Al₂O₃ (1 wt%) as the optimal catalyst, effects of reaction parameters (temperature, pH, pressure and catalyst pretreatment) were studied over extended times (*i.e.*, 6 h) in order to understand and optimize this innovative NADH regeneration process. As seen in **Figure 15**, under benchmark conditions (*i.e.*, 37°C, pH = 7 and 9 atm H₂) the regenerated NADH at the end of reaction achieved 100% selectivity towards the enzymatically active form (~50% yield) and this was confirmed by results from both ¹H NMR (see **Figure S1**) and an independent enzymatic assay (experimental details available from Wang and Yiu¹⁴). In general, high temperature, pH and H₂ pressure favor the reduction of NAD⁺ to NADH (**Figure 16**), which can be related to the activation energy provided (from temperature), driven force for the forward reaction (neutralization of the H⁺ produced, **Figure 5**) and increased H₂ solubility (more reactant available), respectively. Although these observations are promising, it is worth pointing out that high temperature (60 °C) and prolonged reaction time (24 h) can lead to the formation of undesirable products and a loss of cofactor NADH (**Figure 16A**). This tends not to be a problem and has little effect on an actual enzymatic reduction with *in situ* NADH recycling system because it is typically operated at ~37°C or lower temperatures while excessive accumulation of cofactor can be prevented by its concurrent consumption by a substrate over the production enzyme. The *TOFs* (all < 100 h⁻¹) obtained under various conditions are presented in **Figure 16**, suggesting further enhancement would be beneficial. It is also evident that the H₂ treated catalyst is more active than the as-received one (**Figure 16D**), suggesting some differences in their structural characteristics.

Both the as received and H₂ treated catalysts have therefore been fully characterized and the results compiled in **Table 7** and **Figure 17**.¹⁴ There are not significant differences in terms of surface area/porosity and Pt particle size/range (see **Figure 17A** and **17B** for representative STEM images and associated particle size distributions). The H₂ activation capacity evident from both catalysts may be responsible for the reduction of NAD⁺, where the higher (~5 times) value obtained over the H₂ treated catalyst is consistent with the catalytic performance. The X-ray diffraction (XRD) patterns (**Figure 17C**) indicated the presence of PtO₂ in the as received catalyst that was reduced after H₂ treatment. This is consistent with the H₂ temperature programmed reduction (TPR) profile (**Figure 17D**) that the pretreatment at 350°C (for 1 h) is sufficient to reduce all Pt oxide species (see **Supplemental Information** for detailed discussion on the XRD and TPR results). The increased H₂ uptake can therefore be linked to the further reduction of Pt species over the as received catalyst, suggesting metallic Pt is (at least) contains the active site for this reaction.

The ultimate goal for NADH regeneration is to couple this *in situ* with the main enzymatic reaction, which can be challenging due to compatibility issues (as discussed previously in some systems involving organometallic complexes). We have therefore integrated NADH regeneration by Pt/Al₂O₃ with conversion of propanal to propanol over ADH as a model enzymatic redox transformation and the results are shown in **Figure 18**. In batch mode, the production of propanol is limited by the available NADH and without Pt/Al₂O₃ addition propanol yield reached an upper limit of 70%. Cofactor regeneration by Pt/Al₂O₃ extended alcohol production beyond the initial NADH/propanal stoichiometry to reach full conversion (100% yield, **Figure 18A**). Moreover, in order to realize the full potential of this *in situ* cofactor regeneration strategy the feasibility of fed-batch propanol production was investigated using a fixed starting amount of NADH with continuous propanal supply and cofactor regeneration by Pt/Al₂O₃. Without cofactor regeneration, propanol production is limited by the initial NADH

concentration (**Figure 18B**). Propanol production with a continuous feed was achieved through the combined catalytic action of Pt/Al₂O₃ and alcohol dehydrogenase where a constant level of propanol production was maintained in operation for up to 100 h. This hybrid synthetic-biocatalytic system (with further enhancements considered) can serve as a new route for cleaner production of chemicals by NADH dependent enzymes. ~~Promoted~~Prompted by this work, Vincent and coworkers have recently loaded Pt (at a ~~very~~rather high loading, *i.e.*, 20wt%) onto a carbon support to replace hydrogenase and work in tandem with NAD⁺ reductase for NADH regeneration, which has also been proven feasible.¹⁸ This further suggests that supported metals can work with enzymes in “one-pot” and exhibit no mutual inhibition.

These results demonstrate the feasibility of conventional heterogeneous catalysts promoted NAD⁺ reduction by H₂ for the regeneration of NADH, which can be integrated in tandem with a real biotransformation with compatibility. This sixth regeneration method could provide new considerations in both NAD(P)H regeneration technology and the research of heterogeneous catalysis for novel applications.

SUMMARY AND OUTLOOK

NAD(P)H is a critical cofactor that participates in a broad range of enzymatic reduction reactions of both industrial and academic importance. This has been evident from the continuously growing global pharmaceutical market where a significant amount of drugs (or crucial intermediates during production) rely heavily on bioreduction (mainly due to its enantioselectivity) using oxidoreductases as biocatalyst and NAD(P)H as reducing agent. The regeneration of NAD(P)H is necessitated by its high cost and has become a boosting subject of research since ~50 years ago. Overall, six methods have been established to promote NAD(P)⁺ to NAD(P)H transformation, namely enzymatic, chemical, homogeneous catalytic, electrochemical, photochemical and heterogeneous catalytic approaches.

Regeneration using enzymes (notably FDH and GDH) is still the state-of-the-art method and the only one applicable at industrial scale. This is resulted from their high TTN, selectivity to enzymatically active NAD(P)H and excellent compatibility when coupling *in situ* with bioreductions. In addition to some noted limitations of using enzymes (*e.g.*, relatively high cost and low stability), the generation of water soluble byproducts (or CO₂ release), the complexity of species/components involved (*e.g.*, sacrificial organic hydride donor and corresponding byproduct) and product/catalyst separation are concerns towards sustainable and responsible production. This review has thus summarized the advancement of heterogeneous systems for NAD(P)H regeneration across the six categories of methods for potential process simplicity, cleanliness and ease of downstream separation. Except for obsolete chemical regeneration using high redox potential salts, other approaches are (*e.g.*, electro- and heterogeneous catalysis) or can be designed/made (*e.g.*, enzymatic, homogeneous and photo- catalysis) to be heterogeneous. The latter include the demonstrated immobilization of enzymes, organometallic complex and the use of solid photocatalysts. It is unfortunately a common feature that these heterogeneous processes exhibit low activity in NAD(P)⁺ reduction comparing to the homogeneous counterparts, with very few examples achieving high *TOFs*. Nevertheless, they can catalyze selective NAD(P)H regeneration, enhance stability, facilitate catalyst recycling/separation and are compatible in general with *in situ* enzymatic reductions (with various successful examples).

It can also be concluded that using heterogeneous systems do not directly simplify product separation as heterogenized enzymes and organic complex still require sacrificial organic hydride donors while the performance of electrochemical and photochemical routes is strongly dependent on the use of toxic electron mediator in addition to the hydride donors. The critical consideration here is the switch from organic hydride donors to H₂ (preferably from renewable resources) where protons are the single species released and can be consumed in the target

biosynthesis (*i.e.*, 100% atom efficiency). This makes immobilized hydrogenase (with the help of NAD(P)⁺ reductase) and heterogeneous catalysis over supported metals ideal candidates, both of which are proven compatible with enzymatic reductions. Future research in improving the catalytic efficiency is important to fulfill the potential of these two methods in cleaner production of drugs and chemicals. While the hydrogenase/NAD(P)⁺ reductase process is more established, the reaction mechanism of supported metals promoting NAD(P)⁺ reduction is yet clear. An understanding of how NAD(P)⁺ interacts with the catalyst surface, active sites, reaction pathways and energetics will contribute decisively to the rational design of effective catalytic materials. It is hoped that cofactor NAD(P)H regeneration using H₂ over a heterogeneous system can be eventually enhanced to an industrially acceptable level in the future with interdisciplinary efforts from chemists, engineers, biologists and industrial partners.

SUPPLEMENTAL INFORMATION

Supplemental Information includes one figure, experimental details and discussions with associated references.”

AUTHOR CONTRIBUTIONS

X.W. conceived and proposed this work with support from H.H.P.Y. and R.F.H. H.H.P.Y. contributed to the enzymatic regeneration, T.S. contributed to the electrochemical regeneration and J.S. contributed to the photochemical regeneration. X.W. performed the experimental work, wrote the rest sections and was responsible for integrating the article with support from H.H.P.Y. and J.A.A. All authors read, revised and approved the manuscript.

ACKNOWLEDGEMENTS

This work was supported by The Carnegie Trust for the Universities of Scotland (70265), The Royal Society (RG150001 and IE150611) and Scottish Carbon Capture and Storage (SCCS) program. J.S. also acknowledges financial support from The National Natural Science

Foundation of China (21406163 and 91534126). T.S. was supported by a University of Aberdeen Elphinstone PhD Scholarship.

REFERENCES AND NOTES

1. Bornscheuer, U. T., Huisman, G. W., Kazlauskas, R. J., Lutz, S., Moore, J. C., and Robins, K. (2012) Engineering the third wave of biocatalysis. *Nature* **485**, 185-194.
2. Straathof, A. J. J. (2014) Transformation of biomass into commodity chemicals using enzymes or cells. *Chem. Rev.* **114**, 871-1908.
3. Ciriminna, R., and Pagliaro, M. (2013) Green chemistry in the fine chemicals and pharmaceutical industries. *Org. Process. Res. Dev.* **17**, 1479-1484.
4. Hollmann, F., Arends, I. W. C. E., and Holtmann, D. (2011) Enzymatic reductions for the chemist. *Green Chem.* **13**, 2285-2314.
5. Moore, J. C., Pollard, D. J., Kosjek, B., and Devine, P. N. (2007) Advances in the enzymatic reduction of ketones. *Acc. Chem. Res.* **40**, 1412-1419.
6. EvaluatePharma. (2016) World Preview 2016, Outlook to 2022. (9th Edition), pp 9.
7. Gorecki, M. (2015) A configurational and conformational study of (-)-Oseltamivir using a multi-chiroptical approach. *Org. Biomol. Chem.* **13**, 2999-3010.
8. Wu, H., Tian, C., Song, X., Liu, C., Yang, D., and Jiang, Z. (2013) Methods for the regeneration of nicotinamide coenzymes. *Green Chem.* **15**, 1773-1789.
9. Kara, S., Schrittwieser, J., Hollmann, F., and Ansorge-Schumacher, M. (2014) Recent trends and novel concepts in cofactor-dependent biotransformations. *Appl. Microbiol. Biotechnol.* **98**, 1517-1529.
10. Faber, K. (2011) Biocatalytic Applications. in *Biotransformations in Organic Chemistry*, Springer, Berlin/Heidelberg. pp 31-313
11. Hollmann, F., Arends, I. W. C. E., and Buehler, K. (2010) Biocatalytic redox reactions for organic synthesis: nonconventional regeneration methods. *ChemCatChem* **2**, 762-782.
12. Quinto, T., Köhler, V., and Ward, T. (2014) Recent trends in biomimetic NADH regeneration. *Top. Catal.* **57**, 321-331.
13. Poizat, M., Arends, I. W. C. E., and Hollmann, F. (2010) On the nature of mutual inactivation between $[\text{Cp}^*\text{Rh}(\text{bpy})(\text{H}_2\text{O})]^{2+}$ and enzymes—analysis and potential remedies. *J. Mol. Catal. B: Enzym.* **63**, 149-156.
14. Wang, X., and Yiu, H. H. P. (2016) Heterogeneous catalysis mediated cofactor NADH regeneration for enzymatic reduction. *ACS Catal.* **6**, 1880-1886.
15. Ni, Y., and Hollmann, F. (2016) Artificial photosynthesis: Hybrid systems. *Adv.*

- Biochem. Eng. Biotechnol., 1-22.
16. Hollmann, F., Hofstetter, K., and Schmid, A. (2006) Non-enzymatic regeneration of nicotinamide and flavin cofactors for monooxygenase catalysis. *Trends Biotechnol.* **24**, 163-171.
 17. Lauterbach, L., Lenz, O., and Vincent, K. A. (2013) H₂-driven cofactor regeneration with NAD(P)⁺-reducing hydrogenases. *FEBS J.* **280**, 3058-3068.
 18. Reeve, H. A., Ash, P. A., Park, H., Huang, A., Posidias, M., Tomlinson, C., Lenz, O., and Vincent, K. A. (2017) Enzymes as modular catalysts for redox half-reactions in H₂-powered chemical synthesis: from biology to technology. *Biochem. J.* **474**, 215-230.
 19. Liu, W., and Wang, P. (2007) Cofactor regeneration for sustainable enzymatic biosynthesis. *Biotechnol. Adv.* **25**, 369-384.
 20. Goldberg, K., Schroer, K., Lütz, S., and Liese, A. (2007) Biocatalytic ketone reduction-a powerful tool for the production of chiral alcohols-part I: processes with isolated enzymes. *Appl. Microbiol. Biotechnol.* **76**, 237.
 21. Weckbecker, A., Gröger, H., and Hummel, W. (2010) Regeneration of Nicotinamide Coenzymes: Principles and Applications for the Synthesis of Chiral Compounds. in *Biosystems Engineering I: Creating Superior Biocatalysts* (Wittmann, C., and Krull, R. eds.), Springer, Berlin/Heidelberg. pp 195-242
 22. van der Donk, W. A., and Zhao, H. (2003) Recent developments in pyridine nucleotide regeneration. *Curr. Opin. Biotech.* **14**, 421-426.
 23. Wichmann, R., and Vasic-Racki, D. (2005) Cofactor Regeneration at the Lab Scale. in *Technology Transfer in Biotechnology: From lab to Industry to Production* (Kragl, U. ed.), Springer, Berlin/Heidelberg. pp 225-260
 24. Wandrey, C., and Wichmann, R. (1985) Coenzyme regeneration in membrane reactors. in *Enzymes and immobilized cells in biotechnology* (Laskin, A. I. ed.), Benjamin/Cummings Pub. Co., Menlo Park, CA. pp 177-208
 25. Chenault, H. K., and Whitesides, G. M. (1987) Regeneration of nicotinamide cofactors for use in organic synthesis. *Appl. Biochem. Biotech* **14**, 147-197.
 26. Taylor, D. (2016) The Pharmaceutical Industry and the Future of Drug Development. in *Pharmaceuticals in the Environment* (Hester, R. E., and Harrison, R. M. eds.), The Royal Society of Chemistry, Cambridge. pp 1-33
 27. Rafter, G. W., and Colowick, S. P. (1957) Enzymatic preparation of DPNH and TPNH. in *Method. Enzymol.*, Academic Press. pp 887-890
 28. Ferrandi, E. E., Monti, D., and Riva, S. (2014) New Trends in the In Situ Enzymatic Recycling of NAD(P)(H) Cofactors. in *Cascade Biocatalysis*, Wiley-VCH Verlag GmbH & Co. KGaA, Weinheim. pp 23-42

29. De Wildeman, S. M., Sonke, T., Schoemaker, H. E., and May, O. (2007) Biocatalytic reductions: from lab curiosity to 'first choice'. *Acc. Chem. Res.* **40**, 1260-1266.
30. Jones, J. B., Sneddon, D. W., Higgins, W., and Lewis, A. J. (1972) Preparative-scale reductions of cyclic ketones and aldehyde substrates of horse liver alcohol dehydrogenase with in situ sodium dithionite recycling of catalytic amounts of NAD. *Chem. Commun.*, 856-857.
31. Taylor, K. E., and Jones, J. B. (1976) Nicotinamide coenzyme regeneration by dihydropyridine and pyridinium compounds. *J. Am. Chem. Soc.* **98**, 5689-5694.
32. Raunio, R., and Lilius, E. (1971) Effect of dithionite on enzyme activities in vivo. *Enzymologia* **40**, 360.
33. Abril, O., and Whitesides, G. M. (1982) Hybrid organometallic/enzymic catalyst systems: regeneration of NADH using dihydrogen. *J. Am. Chem. Soc.* **104**, 1552-1554.
34. Maenaka, Y., Suenobu, T., and Fukuzumi, S. (2012) Efficient catalytic interconversion between NADH and NAD⁺ accompanied by generation and consumption of hydrogen with a water-soluble iridium complex at ambient pressure and temperature. *J. Am. Chem. Soc.* **134**, 367-374.
35. Maenaka, Y., Suenobu, T., and Fukuzumi, S. (2012) Hydrogen evolution from aliphatic alcohols and 1,4-selective hydrogenation of NAD⁺ catalyzed by a [C,N] and a [C,C] cyclometalated organoiridium complex at room temperature in water. *J. Am. Chem. Soc.* **134**, 9417-9427.
36. Ganesan, V., Sivanesan, D., and Yoon, S. (2017) Correlation between the structure and catalytic activity of [Cp*Rh(substituted bipyridine)] complexes for NADH regeneration. *Inorg. Chem.* **56**, 1366-1374.
37. Bhaduri, S., Mathur, P., Payra, P., and Sharma, K. (1998) Coupling of catalyses by carbonyl clusters and dehydrogenases: reduction of pyruvate to l-lactate by dihydrogen. *J. Am. Chem. Soc.* **120**, 12127-12128.
38. Canivet, J., Süß-Fink, G., and Štěpnička, P. (2007) Water-soluble phenanthroline complexes of rhodium, iridium and ruthenium for the regeneration of NADH in the enzymatic reduction of ketones. *Eur. J. Inorg. Chem.*, 4736-4742.
39. Kohlmann, C., Märkle, W., and Lütz, S. (2008) Electroenzymatic synthesis. *J. Mol. Catal. B: Enzym.* **51**, 57-72.
40. Vasic-Racki, D. (2006) History of Industrial Biotransformations—Dreams and Realities. in *Industrial Biotransformations* (Liese, A., Seelbach, K., and Wandrey, C. eds.), Wiley-VCH Verlag GmbH & Co. KGaA, Weinheim. pp 1-36
41. Sheldon, R. A. (2011) Characteristic features and biotechnological applications of cross-linked enzyme aggregates (CLEAs). *Appl. Microbiol. Biotechnol.* **92**, 467-477.

42. Sheldon, R. A. (2007) Enzyme immobilization: The quest for optimum performance. *Adv. Synth. Catal.* **349**, 1289-1307.
43. Yiu, H. H. P., and Wright, P. A. (2005) Enzymes supported on ordered mesoporous solids: a special case of an inorganic-organic hybrid. *J. Mater. Chem.* **15**, 3690-3700.
44. Kim, J., Grate, J. W., and Wang, P. (2006) Nanostructures for enzyme stabilization. *Chem. Eng. Sci.* **61**, 1017-1026.
45. Sheldon, R. A., and van Pelt, S. (2013) Enzyme immobilisation in biocatalysis: why, what and how. *Chem. Soc. Rev.* **42**, 6223-6235.
46. Wykes, J. R., Dunnill, P., and Lilly, M. D. (1975) Cofactor recycling in an enzyme reactor. A comparison using free and immobilized dehydrogenases with free and immobilized NAD. *Biotechnol. Bioeng.* **17**, 51-68.
47. Danielsson, B., Winqvist, F., Malpote, J. Y., and Mosbach, K. (1982) Regeneration of NADH with immobilized systems of alanine dehydrogenase and hydrogen dehydrogenase. *Biotechnol. Lett.* **4**, 673-678.
48. Ansorge-Schumacher, M. B., Steinsiek, S., Eberhard, W., Keramidas, N., Erkens, K., Hartmeier, W., and Büchs, J. (2006) Assaying CO₂ release for determination of formate dehydrogenase activity in entrapment matrices and aqueous-organic two-phase systems. *Biotechnol. Bioeng.* **95**, 199-203.
49. Binay, B., Alagöz, D., Yildirim, D., Çelik, A., and Tükel, S. S. (2016) Highly stable and reusable immobilized formate dehydrogenases: Promising biocatalysts for in situ regeneration of NADH. *Beilstein J. Org. Chem.* **12**, 271-277.
50. Demir, A. S., Talpur, F. N., Betül Sopacı, S., Kohring, G. W., and Celik, A. (2011) Selective oxidation and reduction reactions with cofactor regeneration mediated by galactitol-, lactate-, and formate dehydrogenases immobilized on magnetic nanoparticles. *J. Biotechnol.* **152**, 176-183.
51. Roche, J., Groenen-Serrano, K., Reynes, O., Chauvet, F., and Tzedakis, T. (2014) NADH regenerated using immobilized FDH in a continuously supplied reactor – application to l-lactate synthesis. *Chem. Eng. J.* **239**, 216-225.
52. Reeve, H. A., Lauterbach, L., Lenz, O., and Vincent, K. A. (2015) Enzyme-modified particles for selective biocatalytic hydrogenation by hydrogen-driven NADH recycling. *ChemCatChem* **7**, 3480-3487.
53. Herr, N., Ratzka, J., Lauterbach, L., Lenz, O., and Ansorge-Schumacher, M. B. (2013) Stability enhancement of an O₂-tolerant NAD⁺-reducing [NiFe]-hydrogenase by a combination of immobilisation and chemical modification. *J. Mol. Catal. B: Enzym.* **97**, 169-174.
54. Horch, M., Lauterbach, L., Lenz, O., Hildebrandt, P., and Zebger, I. (2012) NAD(H)-

- coupled hydrogen cycling–structure–function relationships of bidirectional [NiFe] hydrogenases. *FEBS Lett.* 586, 545-556.
55. Ratzka, J., Lauterbach, L., Lenz, O., and Ansorge-Schumacher, M. B. (2012) Stabilisation of the NAD⁺-reducing soluble [NiFe]-hydrogenase from *Ralstonia eutropha* H16 through modification with methoxy-poly(ethylene) glycol. *J. Mol. Catal. B: Enzym.* 74, 219-223.
 56. El-Zahab, B., Donnelly, D., and Wang, P. (2008) Particle-tethered NADH for production of methanol from CO₂ catalyzed by coimmobilized enzymes. *Biotechnol. Bioeng.* 99, 508-514.
 57. Nagayama, K., Spieß, A. C., and Büchs, J. (2012) Enhanced catalytic performance of immobilized *Parvibaculum lavamentivorans* alcohol dehydrogenase in a gas phase bioreactor using glycerol as an additive. *Chem. Eng. J.* 207–208, 342-348.
 58. Stevenson, E., Ibbotson, P. G., and Spedding, P. L. (1993) Regeneration of NADH in a bioreactor using yeast cells immobilized in alginate fiber: I. Method and effect of reactor variables. *Biotechnol. Bioeng.* 42, 43-49.
 59. Chen, G., Wu, Z., and Ma, Y. (2015) A novel method for preparation of MNP@CS-tethered coenzyme for coupled oxidoreductase system. *J. Biotechnol.* 196–197, 52-57.
 60. Li, Y., Liang, H., Sun, L., Wu, J., and Yuan, Q. (2013) Nanoparticle-tethered NAD⁺ with in situ cofactor regeneration. *Biotechnol. Lett.* 35, 915-919.
 61. de Torres, M., Dimroth, J., Arends, I. W. C. E., Keilitz, J., and Hollmann, F. (2012) Towards recyclable NAD(P)H regeneration catalysts. *Molecules* 17, 9835-9841.
 62. Burnett, J. N., and Underwood, A. L. (1965) Electrochemical reduction of diphosphopyridine nucleotide. *Biochemistry* 4, 2060-2064.
 63. Schmakel, C. O., Santhanam, K. S. V., and Elving, P. J. (1975) Nicotinamide adenine dinucleotide (NAD⁺) and related compounds. Electrochemical redox pattern and allied chemical behavior. *J. Am. Chem. Soc.* 97, 5083-5092.
 64. Baik, S. H., Kang, C., Jeon, I. C., and Yun, S. E. (1999) Direct electrochemical regeneration of NADH from NAD⁺ using cholesterol-modified gold amalgam electrode. *Biotechnol. Tech.* 13, 1-5.
 65. Siu, E., Won, K., and Park, C. B. (2007) Electrochemical regeneration of NADH using conductive vanadia-silica xerogels. *Biotechnol. Progr.* 23, 293-296.
 66. Damian, A., Maloo, K., and Omanovic, S. (2007) Direct electrochemical regeneration of NADH on Au, Cu and Pt-Au electrodes. *Chem. Biochem. Eng. Q.* 21, 21-32.
 67. Ali, I., Soomro, B., and Omanovic, S. (2011) Electrochemical regeneration of NADH on a glassy carbon electrode surface: The influence of electrolysis potential. *Electrochem. Commun.* 13, 562-565.

68. Ali, I., Gill, A., and Omanovic, S. (2012) Direct electrochemical regeneration of the enzymatic cofactor 1,4-NADH employing nano-patterned glassy carbon/Pt and glassy carbon/Ni electrodes. *Chem. Eng. J.* *188*, 173-180.
69. Ali, I., Khan, T., and Omanovic, S. (2014) Direct electrochemical regeneration of the cofactor NADH on bare Ti, Ni, Co and Cd electrodes: the influence of electrode potential and electrode material. *J. Mol. Catal. A: Chem.* *387*, 86-91.
70. Ullah, N., Ali, I., and Omanovic, S. (2015) Direct electrocatalytic reduction of coenzyme NAD⁺ to enzymatically-active 1,4-NADH employing an iridium/ruthenium-oxide electrode. *Mater. Chem. Phys.* *149–150*, 413-417.
71. Chenault, H. K., Simon, E. S., and Whitesides, G. M. (1988) Cofactor regeneration for enzyme-catalysed synthesis. *Biotechnol. Genet. Eng. Rev.* *6*, 221-270.
72. Steckhan, E. (1994) Electroenzymatic synthesis. in *Electrochemistry V* (Steckhan, E. ed.), Springer, Berlin/Heidelberg. pp 83-111
73. Wienkamp, R., and Steckhan, E. (1982) Indirect electrochemical regeneration of NADH by a bipyridinerhodium(i) complex as electron-transfer agent. *Angew. Chem. Int. Ed.* *21*, 782-783.
74. Ruppert, R., Herrmann, S., and Steckhan, E. (1987) Efficient indirect electrochemical in-situ regeneration of NADH: Electrochemically driven enzymatic reduction of pyruvate catalyzed by d-LDH. *Tetrahedron Lett.* *28*, 6583-6586.
75. Vuorilehto, K., Lütz, S., and Wandrey, C. (2004) Indirect electrochemical reduction of nicotinamide coenzymes. *Bioelectrochemistry* *65*, 1-7.
76. Hildebrand, F., Kohlmann, C., Franz, A., and Lütz, S. (2008) Synthesis, characterization and application of new rhodium complexes for indirect electrochemical cofactor regeneration. *Adv. Synth. Catal.* *350*, 909-918.
77. Hildebrand, F., and Lütz, S. (2009) Stable electroenzymatic processes by catalyst separation. *Chem-Eur. J.* *15*, 4998-5001.
78. Tan, B., Hickey, D. P., Milton, R. D., Giroud, F., and Minteer, S. D. (2015) Regeneration of the NADH cofactor by a rhodium complex immobilized on multi-walled carbon nanotubes. *J. Electrochem. Soc.* *162*, H102-H107.
79. DiCosimo, R., Wong, C.-H., Daniels, L., and Whitesides, G. M. (1981) Enzyme-catalyzed organic synthesis: electrochemical regeneration of NAD(P)H from NAD(P) using methyl viologen and flavoenzymes. *J. Org. Chem.* *46*, 4622-4623.
80. Bergel, A., and Comtat, M. (1992) Reduction of NAD(P)⁺ by electrochemically driven FADH₂ and FMNH₂. *J. Electroanal. Chem.* *342*, 495-500.
81. Peguin, S., and Soucaille, P. (1996) Modulation of metabolism of *Clostridium acetobutylicum* grown in chemostat culture in a three-electrode potentiostatic system

- with methyl viologen as electron carrier. *Biotechnol. Bioeng.* *51*, 342-348.
82. Keisuke, U., Asao, N., and Fujio, T. (1990) Investigation on photochemical reduction of NAD⁺ to NADH in liposomal solution. *Chem. Lett.* *19*, 1433-1436.
 83. Shaked, Z. e., Barber, J. J., and Whitesides, G. M. (1981) Combined electrochemical/enzymic method for in situ regeneration of NADH based on cathodic reduction of cyclic disulfides. *J. Org. Chem.* *46*, 4100-4101.
 84. Kim, M.-H., and Yun, S.-E. (2004) Construction of an electro-enzymatic bioreactor for the production of (R)-mandelate from benzoylformate. *Biotechnol. Lett.* *26*, 21-26.
 85. Kashiwagi, Y., Yanagisawa, Y., Shibayama, N., Nakahara, K., Kurashima, F., Anzai, J., and Osa, T. (1997) Preparative, electroenzymatic reduction of ketones on an all components-immobilized graphite felt electrode. *Electrochim. Acta* *42*, 2267-2270.
 86. Yoon, S. K., Chohan, E. R., Kane, C., Tzedakis, T., and Kenis, P. J. A. (2005) Laminar flow-based electrochemical microreactor for efficient regeneration of nicotinamide cofactors for biocatalysis. *J. Am. Chem. Soc.* *127*, 10466-10467.
 87. Cheikhou, K., and Tzedakis, T. (2008) Electrochemical microreactor for chiral syntheses using the cofactor NADH. *AIChE J.* *54*, 1365-1376.
 88. Jayabalan, R., Sathishkumar, M., Jeong, E. S., Mun, S. P., and Yun, S. E. (2012) Immobilization of flavin adenine dinucleotide (FAD) onto carbon cloth and its application as working electrode in an electroenzymatic bioreactor. *Bioresour. Technol.* *123*, 686-689.
 89. Lee, D., Kim, Y. H., and Park, S. (2016) Enzyme electrode platform using methyl viologen electrochemically immobilized on carbon materials. *J. Electrochem. Soc.* *163*, G93-G98.
 90. Magnuson, A., Anderlund, M., Johansson, O., Lindblad, P., Lomoth, R., Polivka, T., Ott, S., Stensjö, K., Styring, S., and Sundström, V. (2009) Biomimetic and microbial approaches to solar fuel generation. *Acc. Chem. Res.* *42*, 1899-1909.
 91. Jordan, P., Fromme, P., Witt, H. T., Klukas, O., Saenger, W., and Krauß, N. (2001) Three-dimensional structure of cyanobacterial photosystem I at 2.5 Å resolution. *Nature* *411*, 909-917.
 92. Nam, D. H., and Park, C. B. (2012) Visible light-driven NADH regeneration sensitized by proflavine for biocatalysis. *ChemBioChem* *13*, 1278-1282.
 93. Kim, J. H., Lee, M., Lee, J. S., and Park, C. B. (2012) Self-assembled light-harvesting peptide nanotubes for mimicking natural photosynthesis. *Angew. Chem. Int. Ed.* *51*, 517-520.
 94. Yadav, R. K., Baeg, J.-O., Oh, G. H., Park, N.-J., Kong, K.-j., Kim, J., Hwang, D. W., and Biswas, S. K. (2012) A photocatalyst–enzyme coupled artificial photosynthesis

- system for solar energy in production of formic acid from CO₂. *J. Am. Chem. Soc.* *134*, 11455-11461.
95. Yadav, R. K., Oh, G. H., Park, N.-J., Kumar, A., Kong, K.-j., and Baeg, J.-O. (2014) Highly selective solar-driven methanol from CO₂ by a photocatalyst/biocatalyst integrated system. *J. Am. Chem. Soc.* *136*, 16728-16731.
 96. Ryu, J., Lee, S. H., Nam, D. H., and Park, C. B. (2011) Rational design and engineering of quantum-dot-sensitized TiO₂ nanotube arrays for artificial photosynthesis. *Adv. Mater.* *23*, 1883-1888.
 97. Lee, S. H., Ryu, J., Nam, D. H., and Park, C. B. (2011) Photoenzymatic synthesis through sustainable NADH regeneration by SiO₂-supported quantum dots. *Chem. Commun.* *47*, 4643-4645.
 98. Jiang, Z., Lü, C., and Wu, H. (2005) Photoregeneration of NADH using carbon-containing TiO₂. *Ind. Eng. Chem. Res.* *44*, 4165-4170.
 99. Shi, Q., Yang, D., Jiang, Z., and Li, J. (2006) Visible-light photocatalytic regeneration of NADH using P-doped TiO₂ nanoparticles. *J. Mol. Catal. B: Enzym.* *43*, 44-48.
 100. Geng, J., Yang, D., Zhu, J., Chen, D., and Jiang, Z. (2009) Nitrogen-doped TiO₂ nanotubes with enhanced photocatalytic activity synthesized by a facile wet chemistry method. *Mater. Res. Bull.* *44*, 146-150.
 101. Liu, J., Huang, J., Zhou, H., and Antonietti, M. (2014) Uniform graphitic carbon nitride nanorod for efficient photocatalytic hydrogen evolution and sustained photoenzymatic catalysis. *ACS Appl. Mater. Interfaces* *6*, 8434-8440.
 102. Liu, J., and Antonietti, M. (2013) Bio-inspired NADH regeneration by carbon nitride photocatalysis using diatom templates. *Energy Environ. Sci.* *6*, 1486-1493.
 103. Huang, J., Antonietti, M., and Liu, J. (2014) Bio-inspired carbon nitride mesoporous spheres for artificial photosynthesis: photocatalytic cofactor regeneration for sustainable enzymatic synthesis. *J. Mater. Chem. A* *2*, 7686-7693.
 104. Liu, J., Cazelles, R., Chen, Z. P., Zhou, H., Galarneau, A., and Antonietti, M. (2014) The bioinspired construction of an ordered carbon nitride array for photocatalytic mediated enzymatic reduction. *Phys. Chem. Chem. Phys.* *16*, 14699-14705.
 105. Dibenedetto, A., Stufano, P., Macyk, W., Baran, T., Fragale, C., Costa, M., and Aresta, M. (2012) Hybrid technologies for an enhanced carbon recycling based on the enzymatic reduction of CO₂ to methanol in water: chemical and photochemical NADH regeneration. *ChemSusChem* *5*, 373-378.
 106. Lee, M., Kim, J. H., Lee, S. H., Lee, S. H., and Park, C. B. (2011) Biomimetic artificial photosynthesis by light-harvesting synthetic wood. *ChemSusChem* *4*, 581-586.
 107. Brown, K. A., Wilker, M. B., Boehm, M., Hamby, H., Dukovic, G., and King, P. W.

- (2016) Photocatalytic regeneration of nicotinamide cofactors by quantum dot–enzyme biohybrid complexes. *ACS Catal.* **6**, 2201-2204.
108. Bhoware, S. S., Kim, K. Y., Kim, J. A., Wu, Q., and Kim, J. (2011) Photocatalytic activity of Pt nanoparticles for visible light-driven production of NADH. *J. Phys. Chem. C* **115**, 2553-2557.
 109. Park, C. B., Lee, S. H., Subramanian, E., Kale, B. B., Lee, S. M., and Baeg, J.-O. (2008) Solar energy in production of l-glutamate through visible light active photocatalyst—redox enzyme coupled bioreactor. *Chem. Commun.*, 5423-5425.
 110. Oppelt, K. T., Gasiorowski, J., Egbe, D. A. M., Kollender, J. P., Himmelsbach, M., Hassel, A. W., Sariciftci, N. S., and Knör, G. (2014) Rhodium-coordinated poly(arylene-ethynylene)-alt-poly(arylene-vinylene) copolymer acting as photocatalyst for visible-light-powered NAD⁺/NADH reduction. *J. Am. Chem. Soc.* **136**, 12721-12729.
 111. Oppelt, K. T., Wöß, E., Stifinger, M., Schöfberger, W., Buchberger, W., and Knör, G. n. (2013) Photocatalytic reduction of artificial and natural nucleotide co-factors with a chlorophyll-like tin-dihydroporphyrin sensitizer. *Inorg. Chem.* **52**, 11910-11922.
 112. Schneider, J., Matsuoka, M., Takeuchi, M., Zhang, J., Horiuchi, Y., Anpo, M., and Bahnemann, D. W. (2014) Understanding TiO₂ photocatalysis: mechanisms and materials. *Chem. Rev.* **114**, 9919-9986.
 113. Sagawa, T., Sueyoshi, R., Kawaguchi, M., Kudo, M., Ihara, H., and Ohkubo, K. (2004) Photosensitized NADH formation system with multilayer TiO₂ film. *Chem. Commun.*, 814-815.
 114. Eley, C., Li, T., Liao, F., Fairclough, S. M., Smith, J. M., Smith, G., and Tsang, S. C. E. (2014) Nanojunction-mediated photocatalytic enhancement in heterostructured CdS/ZnO, CdSe/ZnO, and CdTe/ZnO nanocrystals. *Angew. Chem. Int. Ed.* **53**, 7838-7842.
 115. Ong, W.-J., Tan, L.-L., Ng, Y. H., Yong, S.-T., and Chai, S.-P. (2016) Graphitic carbon nitride (g-C₃N₄)-based photocatalysts for artificial photosynthesis and environmental remediation: Are we a step closer to achieving sustainability? *Chem. Rev.* **116**, 7159-7329.
 116. Irfan, M., Petricci, E., Glasnov, T. N., Taddei, M., and Kappe, C. O. (2009) Continuous flow hydrogenation of functionalized pyridines. *Eur. J. Org. Chem.* **2009**, 1327-1334.
 117. Song, H.-K., Lee, S. H., Won, K., Park, J. H., Kim, J. K., Lee, H., Moon, S.-J., Kim, D. K., and Park, C. B. (2008) Electrochemical regeneration of NADH enhanced by platinum nanoparticles. *Angew. Chem. Int. Ed.* **47**, 1749-1752.

Tables:

Table 1. Typical Main Criteria Required for Cofactor NAD(P)H Regeneration

Method	Recycling catalyst (ease of separation)	Avoiding organic sacrificial electron donor	Avoiding mediator	Clean production without byproduct
Enzymatic	✗ ✓ (immobilized enzyme)	✗ ✓ (using H ₂)	✓	✗ ✓ (producing H ⁺)
Chemical	– (no catalyst)	✓ (inorganic)	✓	✗
Homogeneous Catalytic	✗	✗ ✓ (using H ₂)	✗	✗ ✓ (producing H ⁺)
Electrochemical	✓	✓	✗ ✓ (nonselective)	✗ ✓ (using me)
Photochemical	✗ (organic photosensitizers) ✓ (inorganic photosensitizers)	✗ ✓ (using H ₂ O)	✗ ✓ (C ₃ N ₄ , only 1 example)	✗
Heterogeneous Catalytic	✓	✓ (using H ₂)	✓	✓ (producing H ⁺)

Table 2. Characteristics of Enzymes Used in Cofactor NAD(P)H Regeneration

Enzyme	Substrate(s)	Byproduct(s) from regeneration	Advantages	Disadvantages
Alcohol dehydrogenase (ADH)	2-propanol (or other oxidizable alcohols)	Acetone (correspondent ketones/aldehydes)	<ul style="list-style-type: none">• High activity• Low cost	<ul style="list-style-type: none">• Water soluble byproducts requiring downstream separation
Formate dehydrogenase (FDH)	Formate/formic acid	CO ₂	<ul style="list-style-type: none">• No soluble byproducts• Enhanced product separation	<ul style="list-style-type: none">• Low activity• CO₂ release
Glucose dehydrogenase (GDH)	Glucose	D-glucono-1,5-lactone	<ul style="list-style-type: none">• High activity	<ul style="list-style-type: none">• High cost• Water soluble byproducts requiring downstream separation
Glutamate dehydrogenase (GLDH)	Glutamate/glutamic acid	γ-aminobutyric acid	<ul style="list-style-type: none">• Low cost	<ul style="list-style-type: none">• Low activity• Water soluble byproducts requiring downstream separation
Hydrogenase	H ₂	H ⁺	<ul style="list-style-type: none">• Clean byproducts (H⁺)	<ul style="list-style-type: none">• Low stability compared with other enzymes• Commercial availability

Table 3. Direct Electrochemical Regeneration of Cofactor NAD(P)H

Electrode	Potential (V)	Cofactor	Results
Au amalgam ⁶⁴	-1.4 vs Ag/AgCl	NAD ⁺	NADH yield = 10%
Pt using vanadia-silica xerogels ⁶⁵	2 ^a	NAD ⁺	NADH yield = 100%; α -ketoglutarate conversion = 100%; time = 3 h.
Au ⁶⁶	-1.1 vs SCE ^b	NAD ⁺	NADH yield = 29.6%
Cu ⁶⁶	-1.2 vs SCE ^b	NAD ⁺	NADH yield = 52%
Pt-Au ⁶⁶	-1.1 vs SCE ^b	NAD ⁺	NADH yield = 63%
GC ⁶⁷	-2.3 vs MSE ^c	NAD ⁺	NADH yield = 98%; time = 3.5 h.
GC-Pt ⁶⁸	-1.6 vs MSE ^c	NAD ⁺	NADH yield = 100%; time = 6 h.
GC-Ni ⁶⁸	-1.5 vs MSE ^c	NAD ⁺	NADH yield = 100%
Ti ⁶⁹	-0.8 vs NHE ^d	NAD ⁺	NADH yield = 96%
Ni ⁶⁹	-1.3 vs NHE ^d	NAD ⁺	NADH yield = 92%
Co ⁶⁹	-0.9 vs NHE ^d	NAD ⁺	NADH yield = 82%
Cd ⁶⁹	-1.5 vs NHE ^d	NAD ⁺	NADH yield = 93%
Ir-Ru/Ti ⁷⁰	-1.7 vs MSE ^c	NAD ⁺	NADH yield = 88%; time = 6 h 40 min.

^a2 V electricity applied.^bSaturated Calomel Electrode.^cMercurous Sulfate Electrode.^dNormal Hydrogen Electrode.

Table 4. Indirect Electrochemical Regeneration of Cofactor NAD(P)H

Electrode	Potential (V)	Redox Catalyst/Mediator	Cofactor	Results
Carbon foil ⁷³	-0.7 vs Ag/AgCl	[Rh(bpy) ₃] ²⁺	NAD ⁺	Cyclohexanone conversion = 26%; TTN _{Cofactor} ^a = 2.9; TTN _{Catalyst} ^b = 1.2
Carbon foil ⁷⁴	-0.6 vs Ag/AgCl	[Cp(Me) ₅ Rh(bipy)Cl] ⁺	NAD ⁺	Pyruvate conversion = 70%; ee = 93.5%; TTN _{Cofactor} ^a = 14; TTN _{Catalyst} ^b = 7
Glassy carbon particles ⁷⁵	-0.5 vs NHE	(pentamethylcyclo-pentadienyl-2,2'-bipyridine aqua) Rh III	NAD ⁺ NADP ⁺	NADH yield = 99.5%; TTN _{Catalyst} ^b = 400 NADPH yield = 99.5%; TTN _{Catalyst} ^b = 200
Carbon felt ⁷⁶	-0.756 vs Ag/AgCl	Cp[Rh(5,5'-methyl-2,2'-bipyridine)]	NADP ⁺	r _{reduction} = 116 mM d ⁻¹ ; TOF = 97 h ⁻¹
	-0.757 vs Ag/AgCl	Cp[Rh(4,4'-methoxy-2,2'-bipyridine)]	NADP ⁺	r _{reduction} = 136 mM d ⁻¹ ; TOF = 113 h ⁻¹
Glassy carbon ⁷⁷	-0.8 vs Ag/AgCl	Rh-polymeric mediator	NADP ⁺	<i>p</i> -chloroacetophenone conversion = 90%; ee > 97.3%; TTN _{Catalyst} ^b = 214
MWCNs ⁷⁸	-0.75 vs SCE	Pyr-Rh	NAD ⁺	TOF = 3.6 s ⁻¹ over 10 regeneration cycles

^aCofactor total turnover number (mol of product produced per mol of cofactor used).^bCatalyst total turnover number (mol of product produced per mol of catalyst used).

Table 5. Enzyme-coupled Indirect Electrochemical Regeneration of Cofactor NAD(P)H

Electrode	Potential (V)	Mediator	Enzyme	Cofactor	Results
Coiled W wire ⁷⁹	-0.72 vs SCE	Methyl viologen (MV)	LipDH	NAD ⁺	TTN _{Cofactor} ^a = 940; TTN _{Enzyme} ^b = 540,000; reaction time = 9 days
			FDR	NADP ⁺	TTN _{Cofactor} ^a = 1000; TTN _{Enzyme} ^b = 750,000; reaction time = 7 days
Coiled W wire ⁸³	-1 vs SCE	Dithiols (DTT)	LipDH	NAD ⁺	TTN _{Cofactor} ^a = 920; TTN _{Enzyme} ^b = 13; reaction time = 3.5 days
Modified graphite ⁸⁴	-0.8 vs SCE	Methyl viologen (MV)	Diaphorase	NAD ⁺	Benzoylformate conversion = 95%; reaction time = 18 h Benzoylformate conversion = 80%; reaction time = 30 h; (50% loss of MV activity after 6 d)
Au amalgam ⁸⁵	-0.5 vs Ag/AgCl	Flavine adenine dinucleotide (FAD)	Diaphorase	NAD ⁺	2-methylcyclohexanone conversion = 49.8%; ee = 100%; TTN _{Mediator} ^c = 91
	-0.7 vs Ag/AgCl	Methyl viologen (MV)			3-methylcyclohexanone conversion = 51.7%; ee = 93.1%; TTN _{Mediator} ^c = 94
Au ⁸⁶	-0.55 vs Pt	Flavine adenine dinucleotide (FAD)	FDH	NAD ⁺	NADH yield = 31%; Pyruvate conversion = 41%; TN = 75.6 h ⁻¹ .
Au ⁸⁷	-0.6 vs Pt				NADH yield = 50%; Pyruvate conversion = 20%; TN = 80 h ⁻¹ .
Unmodified carbon cloth ⁸⁸	-0.45 vs Ag/AgCl	Flavine adenine dinucleotide (FAD)	FDH	NAD ⁺	Pyruvate conversion = 50%; reaction time = 120 h
Modified carbon cloth ⁸⁸	-0.45 vs Ag/AgCl	Immobilized FAD			Pyruvate conversion = 60%; reaction time = 96 h

^aCofactor total turnover number (mol of product produced per mol of cofactor used).

^bEnzyme total turnover number (mol of product produced per mol of enzyme used).

^cMediator total turnover number (mol of product produced per mol of mediator used).

Table 6. Photocatalytic Regeneration of Cofactor NAD(P)H by Selective Heterogeneous Photosensitizers: Summary of Reaction Conditions and Catalytic Performance

Photosensitizer	Electron donor	M ^a	λ (nm)	pH	Yield (%)	TOF (h ⁻¹)
Light-harvesting synthetic wood ¹⁰⁶	TEOA	yes	≥ 400	7.4	4.30	1.250
Pt-doped peptide nanotubes ⁹³	TEOA	yes	≥ 400	6.0	17.80	1.780
CCGCMAQSP ⁹⁴	TEOA	yes	≥ 420	7.0	45.54	0.375
CCG-IP ⁹⁵	TEOA	yes	≥ 420	7.0	38.99	0.642
Rh-BipyE-PVab polymer ¹¹⁰	TEOA	yes	≥ 390	8.9	21.00	1.8 ^b
Carbon-doped TiO ₂ ⁹⁸	Mercaptoethanol	yes	≥ 400	6.5	74.30	0.031
	H ₂ O	yes	≥ 400	6.0	63.98	0.011
Phosphorus-doped TiO ₂ ⁹⁹	H ₂ O	yes	≥ 400	6.5	34.60	0.006
CdS-coated SiO ₂ ⁹⁷	TEOA	yes	≥ 420	7.5	70.00	0.278
CdS-TiO ₂ nanotubular film ⁹⁶	TEOA	yes	≥ 420	7.5	75.20	240 ^b
Diatom-mimic structure (g-C ₃ N ₄) ¹⁰²	TEOA	yes	≥ 420	8.0	100	0.067
	TEOA	no	≥ 420	10.0	50.00	0.248
Porous nanospheres (g-C ₃ N ₄) ¹⁰³	TEOA	yes	≥ 420	8.0	100	1.326
	TEOA	no	≥ 420	10.0	50.00	0.665
Porous nanorods (g-C ₃ N ₄) ¹⁰¹	TEOA	yes	≥ 420	8.0	72.00	0.478

^aM: mediator [Cp^{*}Rh(bpy)H₂O]²⁺ that shows high specificity to enzymatically active NAD(P)H.

^bThe unit of these values is $\mu\text{mol cm}^{-2} \text{h}^{-1}$.

Table 7. Physicochemical Characteristics of Pt/Al₂O₃¹⁴

	Pt/Al ₂ O ₃ (as received)	Pt/Al ₂ O ₃ (H ₂ treated)
BET surface area (m ² g ⁻¹)	162	175
Total pore volume (cm ³ g ⁻¹)	0.40	0.43
Average pore size (nm)	7.8	8.0
Pt size range (nm)	0-7	0-10
<i>d</i> _{STEM} (nm)	2.2	3.4
H ₂ chemisorption (μmol g ⁻¹)	4.1	21.5

Figures:

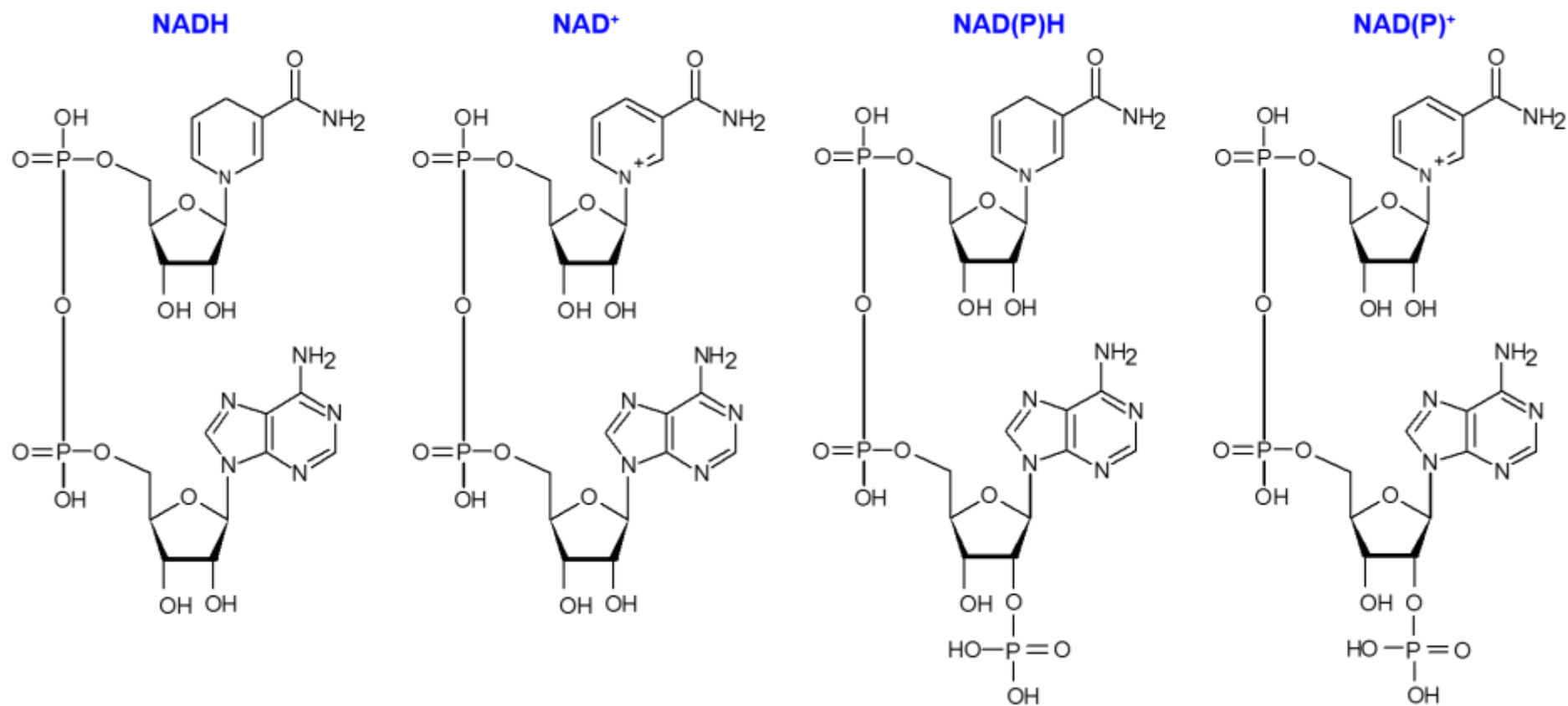


Figure 1. Molecular Structures of Nicotinamide Adenine Dinucleotide Cofactors

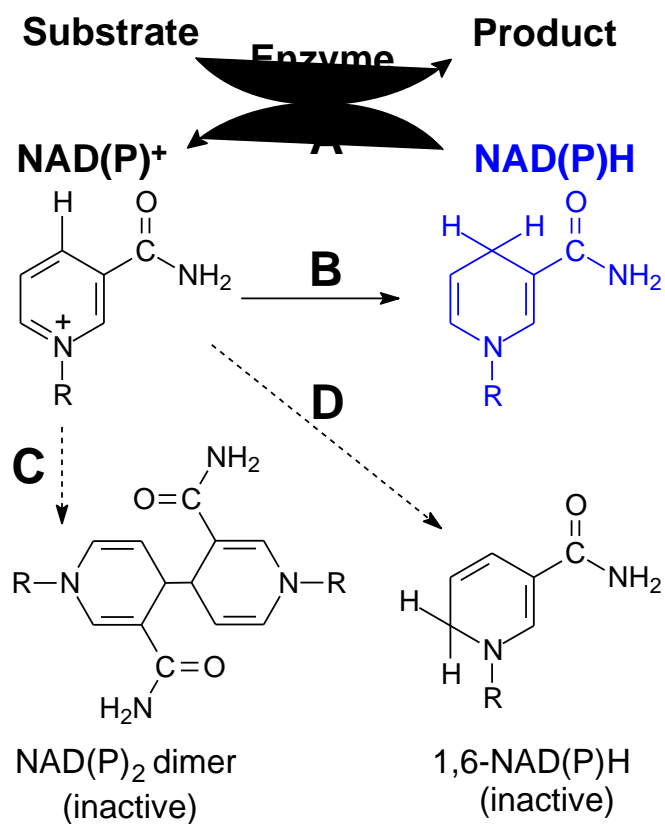


Figure 2. Schematic Representation of Enzymatic Reaction using Cofactor NAD(P)H and Possible Products Obtained from NAD(P)H Regeneration

(A) NAD(P)H consumption in biotransformation.

(B) Target pathway for NAD(P)H regeneration.

(C) Formation of (dashed arrows) enzymatically inactive NAD(P)₂ dimer.

(D) Formation of (dashed arrows) enzymatically inactive 1,6-NAD(P)H.

R indicates adenosine diphosphoribose.

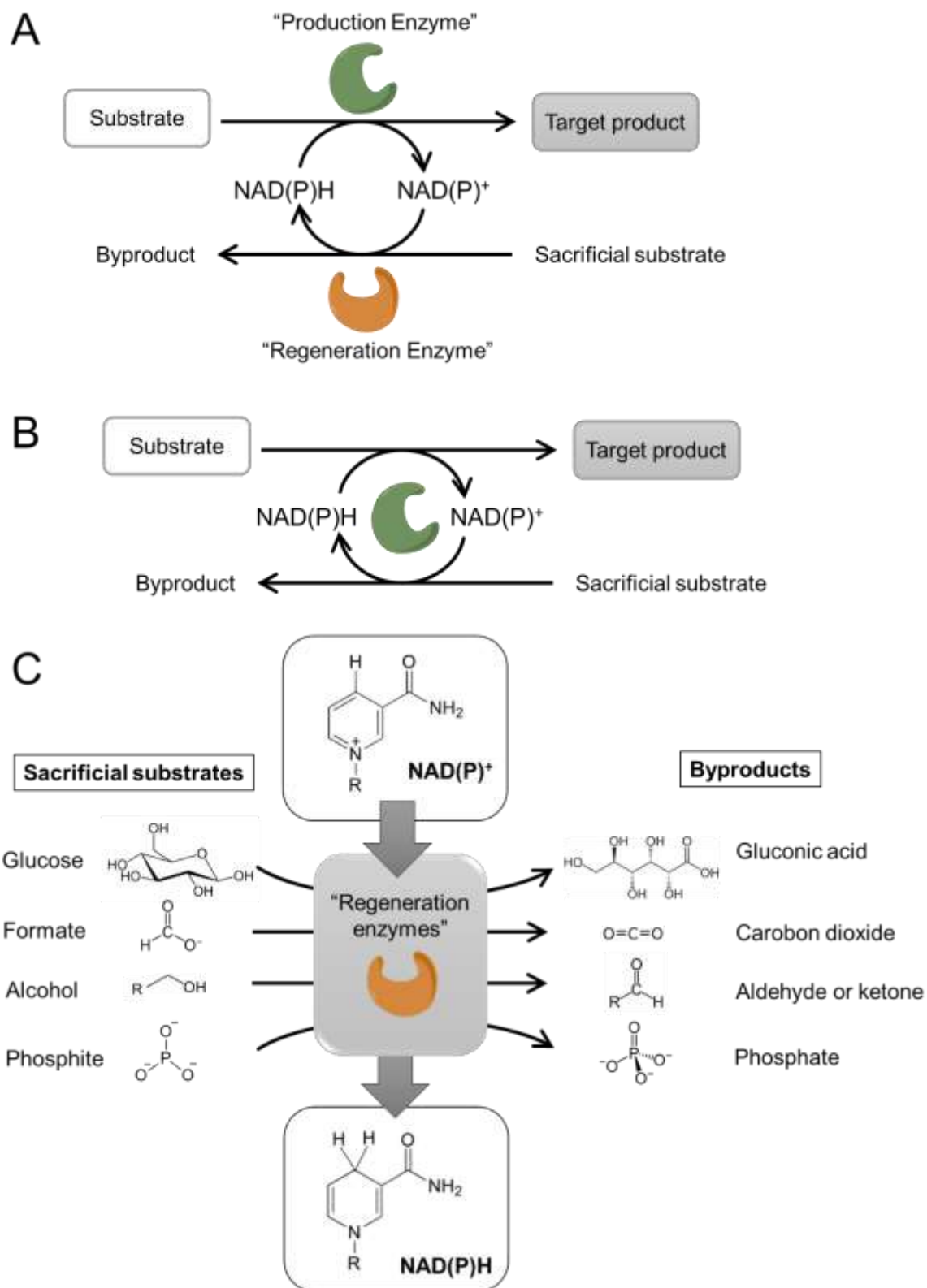


Figure 3. Schematic Representation of NAD(P)H Enzymatic Regeneration

(A) Coupled-enzyme approach.

(B) Coupled-substrate approach.

(C) Typical sacrificial substrates in enzymatic regeneration.

R indicates adenosine diphosphoribose.

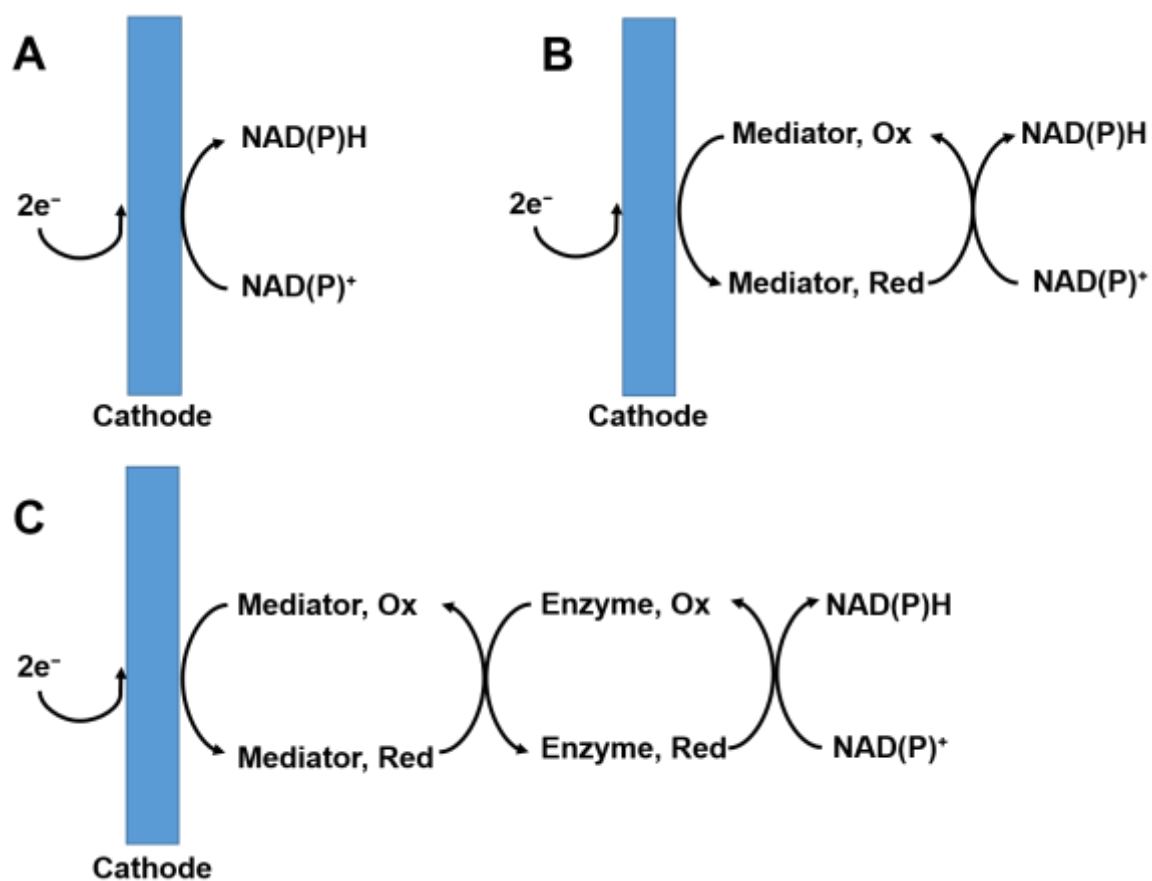
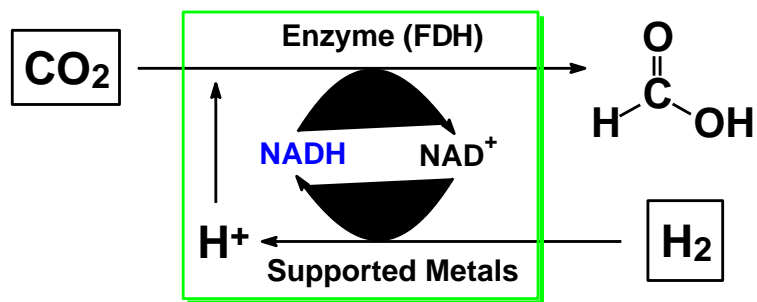


Figure 4. Schematic Representation of NAD(P)H Electrochemical Regeneration

- (A) Direct electrochemical regeneration.
- (B) Indirect electrochemical regeneration.
- (C) Enzyme-coupled electrochemical regeneration.



Reactions involved:

- (1) $\text{NAD}^+ + \text{H}_2 \rightleftharpoons \text{NADH} + \text{H}^+$
- (2) $\text{CO}_2 + \text{NADH} + \text{H}^+ \rightleftharpoons \text{HCOOH} + \text{NAD}^+$
- (3) $\text{CO}_2 + \text{H}_2 \rightleftharpoons \text{HCOOH}$ (overall reaction)

Figure 5. Schematic Representation of Coupling Heterogeneous Catalysts Promoting NADH Regeneration in Tandem with Enzymatic Reduction Using CO₂ as A Representative Substrate (Producing Formic Acid)

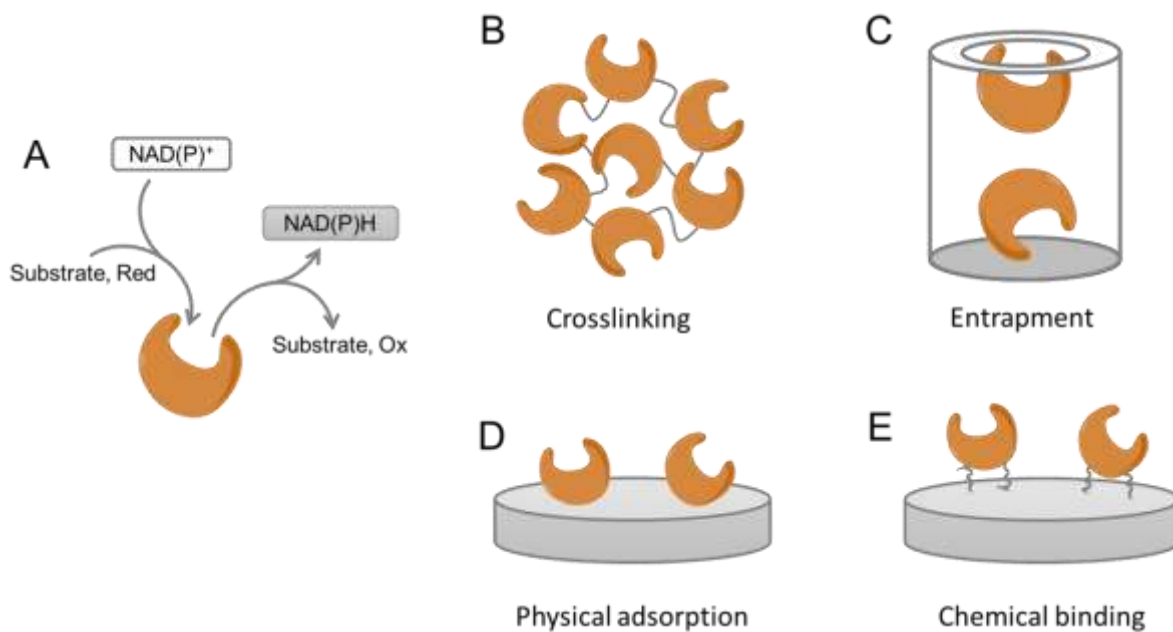


Figure 6. Methods for Enzyme Immobilization

(A) Illustration of enzymatic NAD(P)H regeneration

(B) Crosslinking

(C) Entrapment

(D) Physical adsorption

(E) Chemical binding

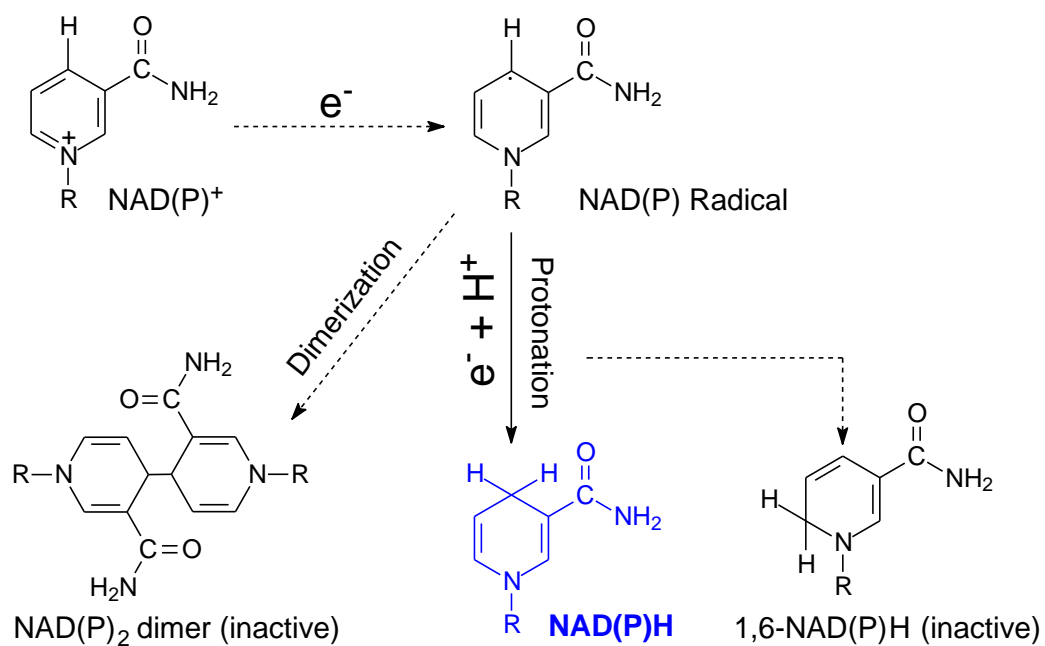


Figure 7. Reaction Pathways in Electrochemical Reduction of NAD(P)⁺ to NAD(P)H.

R indicates adenosine diphosphoribose.

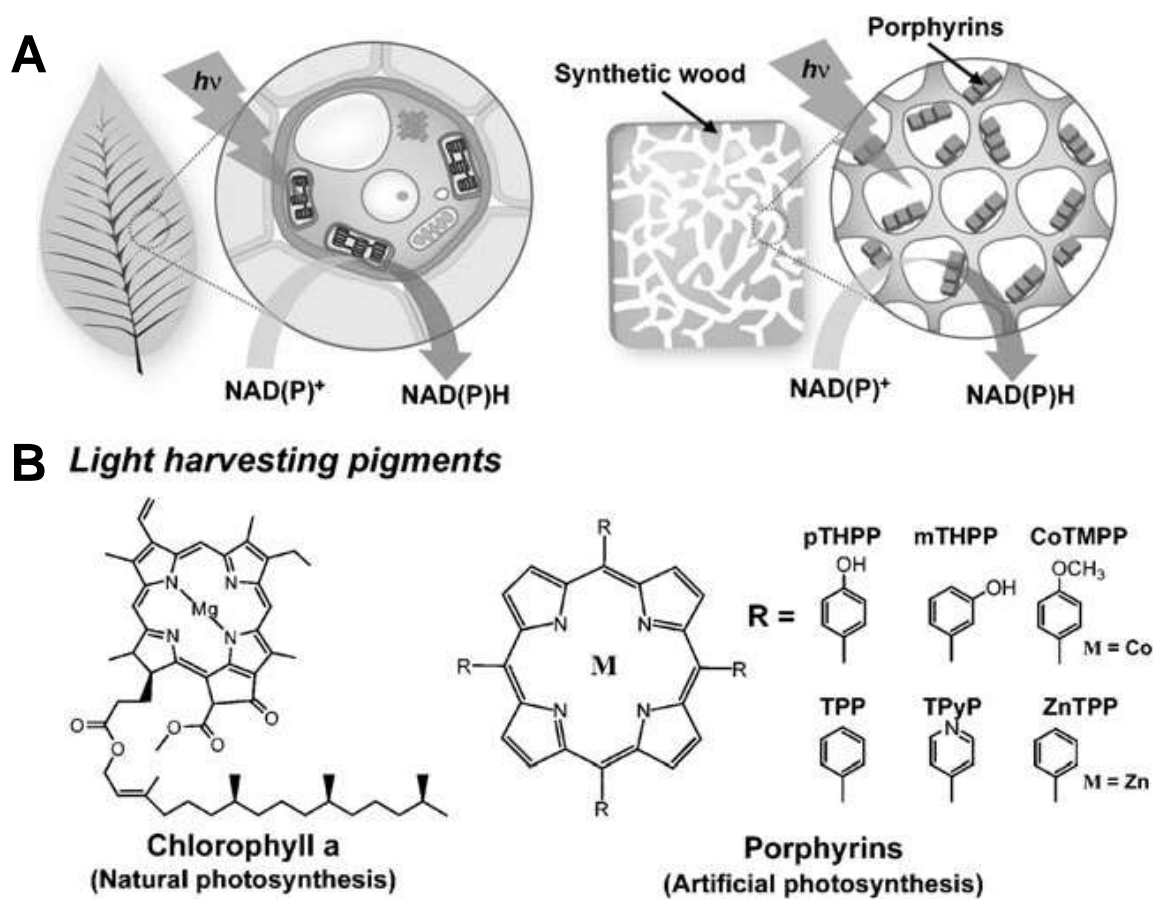


Figure 8. (A) Schematic illustration of the light-harvesting system in green plants (left) and light-harvesting synthetic wood (LSW) (right). (B) Molecular structures of light-harvesting pigment in green plants (left) and LSW (right). Adapted from Lee *et al.*¹⁰⁶ with permission from the 2011 John Wiley & Sons Inc.

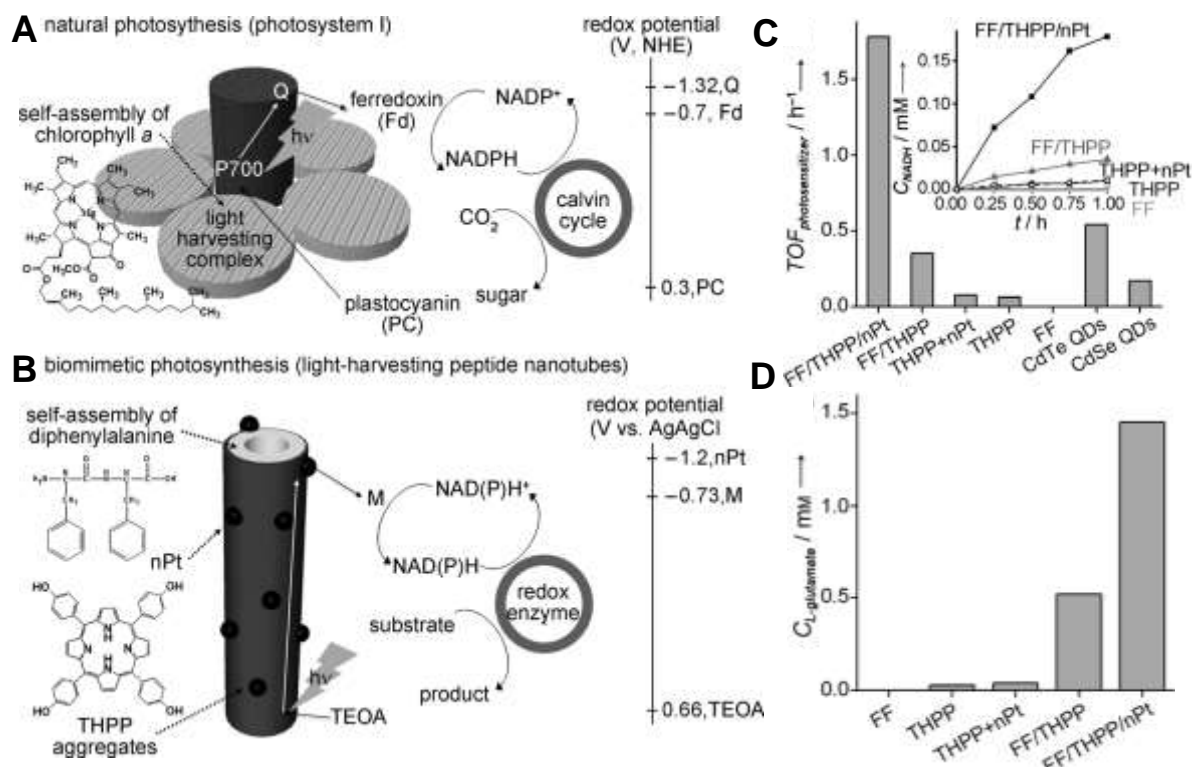


Figure 9. Schematic illustration of (A) structure, biocatalytic reaction, and redox potential of natural photosynthesis by photosystem I and (B) artificial photosynthesis by light-harvesting Pt-doped peptide nanotubes. (C) Turnover frequency of different types of nanotubes in comparison with other inorganic photosensitizers. Inset in (C) shows the temporal change of NADH concentration in the presence of different nanotubes. D) Photosynthesis of L-glutamate by glutamate dehydrogenase (GDH) with different types of nanotubes. Adapted from Kim *et al.*⁹³ with permission from the 2012 John Wiley & Sons Inc.

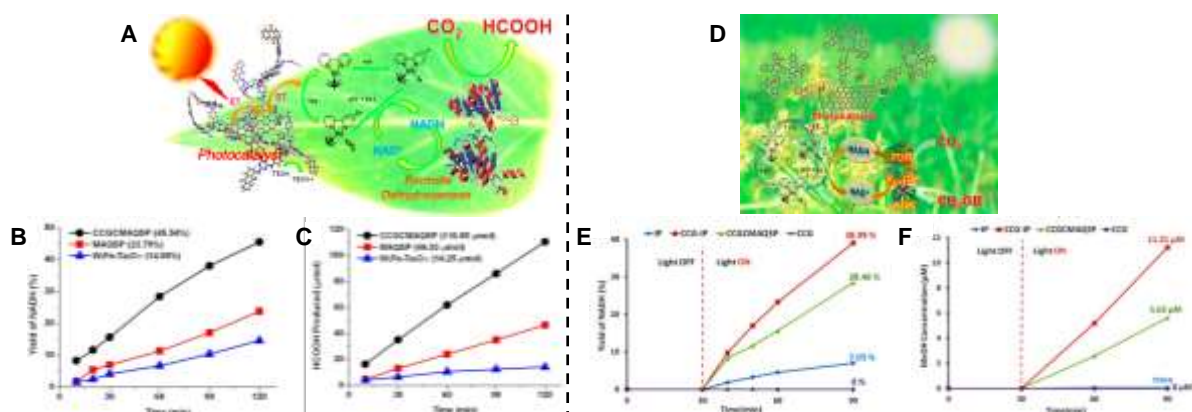


Figure 10. (A) CCGCMAQSP-bonded graphene nanosheet photocatalyzed regeneration of NADH and artificial photosynthesis of formic acid From CO₂ under visible light. (B, C) Photocatalytic activities of CCGCMAQSP and other two photosensitizers in visible-light driven (B) NADH photocatalytic regeneration and (C) artificial photosynthesis of formic acid from CO₂. Adapted from Yadav *et al.*⁹⁴ with permission from the 2012 American Chemical Society. (D) CCGC-IP-bonded graphene nanosheet photocatalyzed regeneration of NADH and artificial photosynthesis of methanol from CO₂ under visible light. (E, F) Photocatalytic activities of CCGC-IP and other two photosensitizers in visible-light driven (E) NADH photocatalytic regeneration and (F) artificial photosynthesis of methanol from CO₂. Adapted from Yadav *et al.*⁹⁵ with permission from the 2014 American Chemical Society.

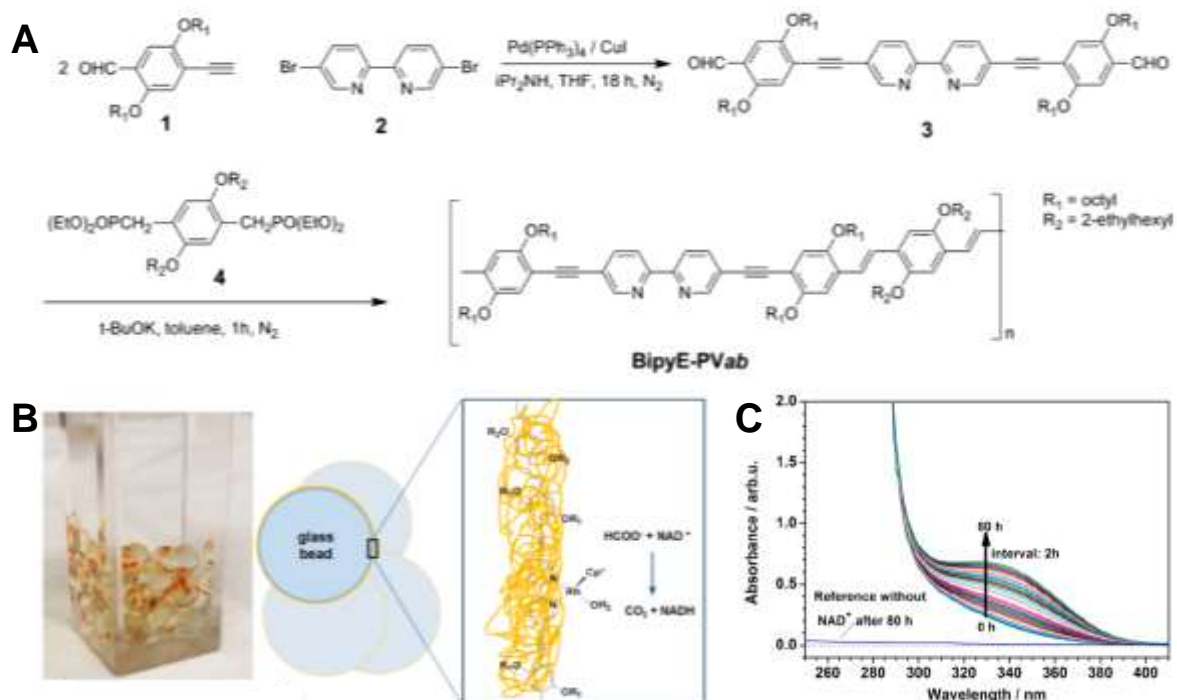


Figure 11. (A) Synthesis procedure of the bipyridine-containing polymer (*bipyridine-containing poly-(arylene-ethynylene)-alt-poly(arylene-vinylene) copolymer*). (B) Experimental setup (left) and scheme of the surface reaction (right) in the chemical reduction of NAD^+ to NADH with formate as hydride donor to the polymer-bound rhodium catalyst reaction center. (C) UV-vis spectra of the chemical reduction of NAD^+ with formate. Adapted from Oppelt *et al.*¹¹⁰ with permission from the 2014 American Chemical Society.

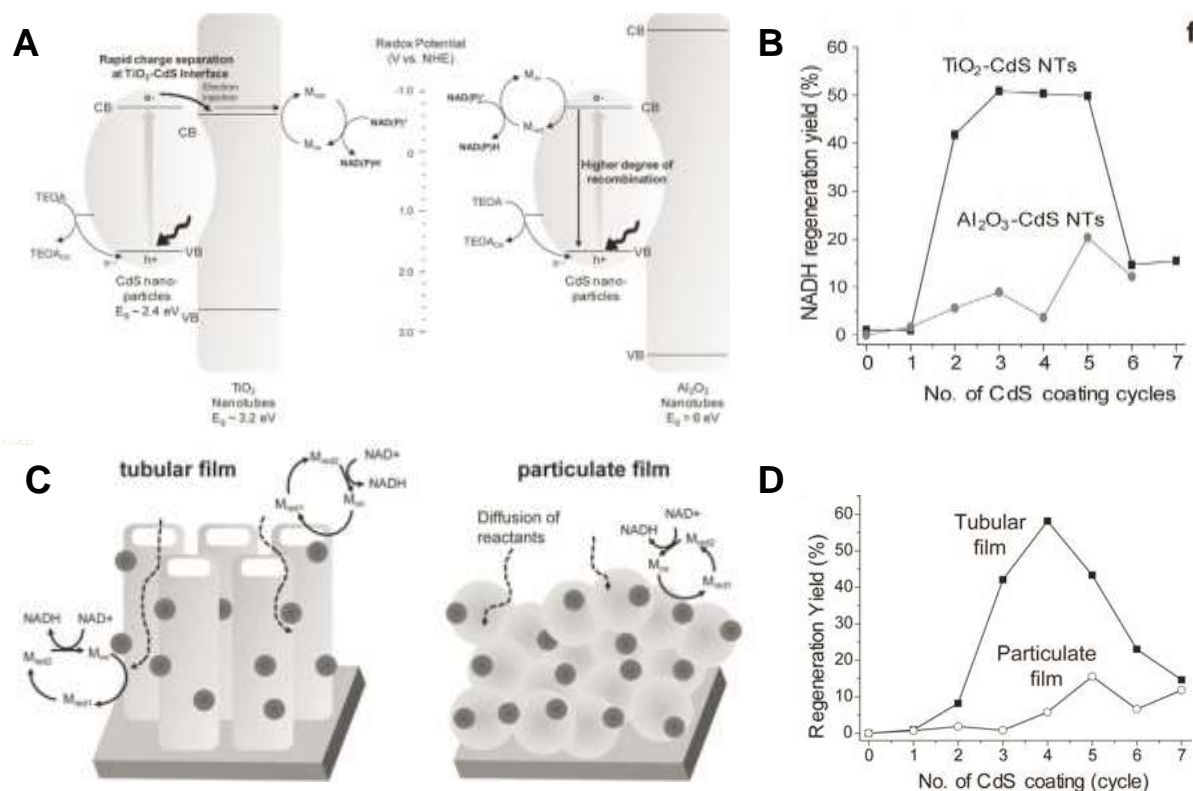


Figure 12. (A) Proposed mechanism for higher efficiency of NADH photocatalytic regeneration by CdS-TiO₂ nanotubular film than CdS-Al₂O₃ nanotubular film. (B) Comparison between the NADH regeneration efficiencies enabled by CdS-TiO₂ nanotubular film and CdS-Al₂O₃ nanotubular film with different degrees of CdS loading. Adapted from Ryu *et al.*⁹⁶ with permission from the 2011 John Wiley & Sons Inc.

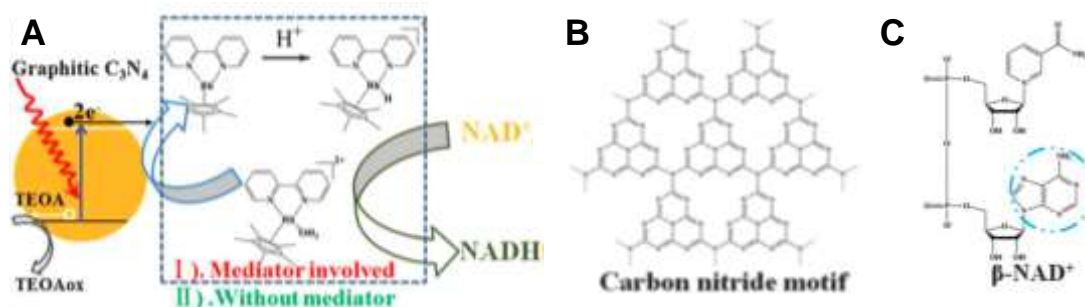


Figure 13. (A) Schematic illustration of photocatalytic regeneration of NADH in the absence or presence of electron mediator. (B and C) Schematic illustration of the interaction between g- C_3N_4 and NAD^+ . (B) Illustration of g- C_3N_4 constructed from heptazine building blocks. (delete C?) Adapted from Liu *et al.*¹⁰² with permission from the 2013 Royal Society of Chemistry.

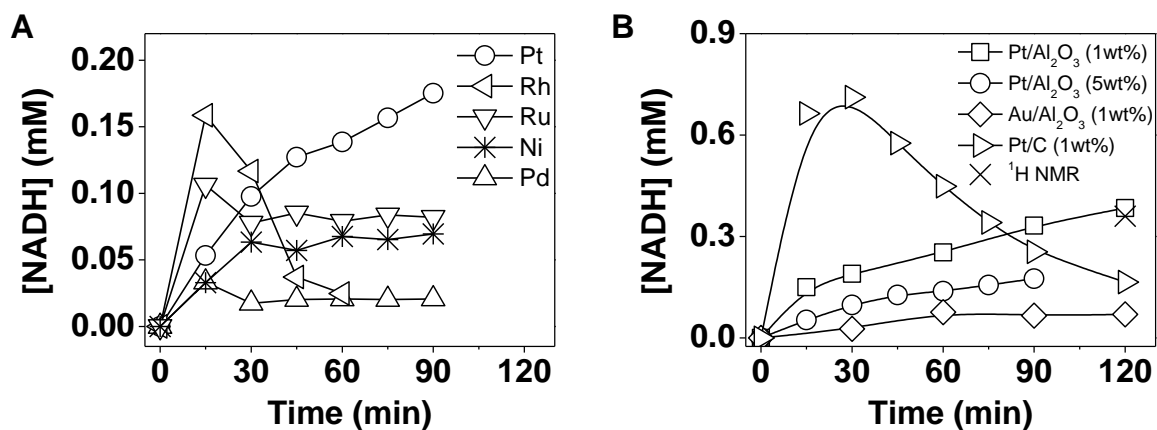


Figure 14. Heterogeneous Catalysts Promoted NADH Regeneration by the Reduction of NAD^+ Using H_2

Variation of NADH concentration as a function of time over (as received) Al_2O_3 supported: (A) 5 wt% Pt (○), Rh (◁), Ru (▽), Pd (△) and (homemade) 6 wt% Ni (*).

(B) 1 wt% Pt/ Al_2O_3 (□), Pt/C (▷), Au/ Al_2O_3 (◇) and 5 wt% Pt/ Al_2O_3 (○) with NADH concentration determined by ^1H NMR (×).

Reaction conditions: $T = 37^\circ\text{C}$, $P = 9\text{ atm}$, $\text{pH} = 7$, $[\text{NAD}^+]_0 = 1.5\text{ mM}$ and 25 mg catalyst.

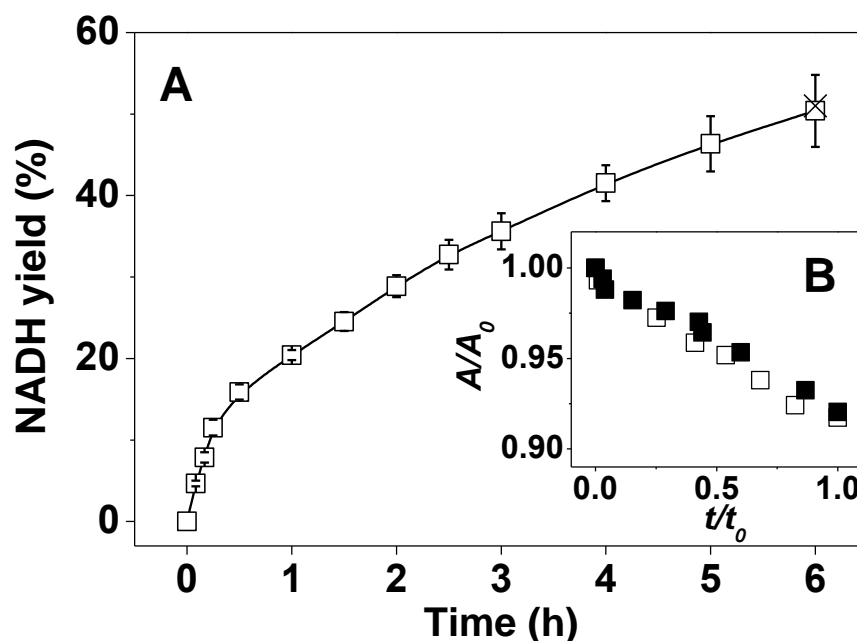


Figure 15. Pt/Al₂O₃ (1 wt%) Catalyzed NAD⁺ Reduction for NADH Regeneration

(A) Variation of NADH yield as a function of time (□) with NADH yield determined by ¹H NMR (×).

(B) NADH yield validation using enzymatic assay (EC 1.8.1.4): time dependence of normalized absorbance (A/A_0) of NADH produced experimentally (□) and from a prepared mixture using commercial NADH and NAD⁺ (■): A_0 is the absorbance recorded before the enzymatic assay; A is the absorbance recorded after reaction is initiated; t_0 is the total run time of the enzymatic assay; t is the time after initiating the reaction.

Reaction conditions: $T = 37\text{ }^{\circ}\text{C}$, $P = 9\text{ atm}$, $\text{pH} = 7$, $[\text{NAD}^+]_0 = 1.5\text{ mM}$ and 25 mg catalyst.

Adapted from Wang and Yiu.¹⁴ with permission from the 2016 American Chemical Society.

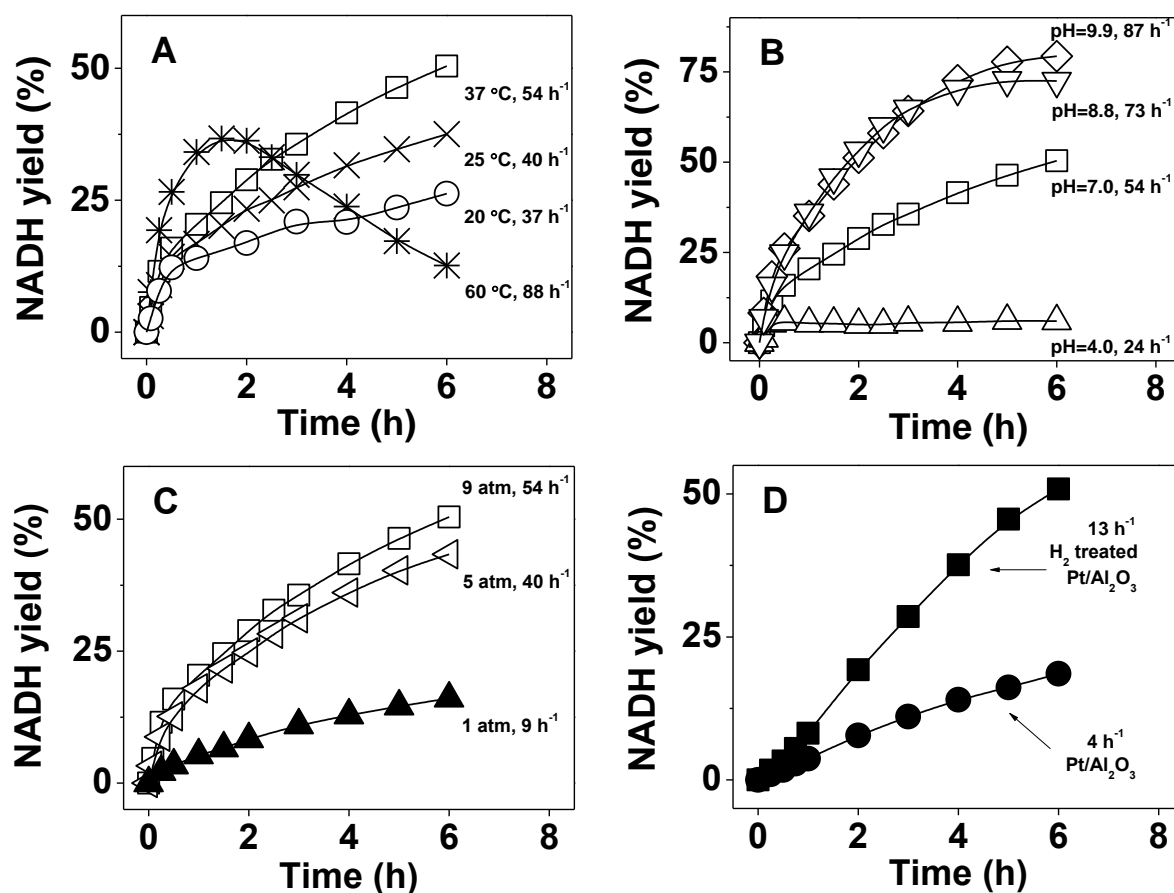


Figure 16. Temporal Variation of NADH Yield and Initial Turnover Frequency (TOF , h^{-1}) As A Function of Reaction Parameters in Pt/Al₂O₃ (1 wt%) Catalyzed NAD⁺ Reduction for NADH regeneration

(A) Temperature (20 °C (○), 25 °C (×), 37 °C (□) and 60 °C (*)) at $P = 9$ atm, $\text{pH} = 7.0$.

(B) pH (4.0 (△), 7.0 (□), 8.8 (▽) and 9.9 (◇)) at $T = 37$ °C, $P = 9$ atm).

(C) Pressure, (1 atm (▲), 5 atm (◁) and 9 atm (□)) at $T = 37$ °C, $\text{pH} = 7.0$.

(D) H₂ treatment (Pt/Al₂O₃ as received (●) and H₂ treated Pt/Al₂O₃ (■)) at $T = 20$ °C, $P = 1$ atm, $\text{pH} = 8.8$.

Reaction conditions: $[\text{NAD}^+]_0 = 1.5$ mM and 25 mg catalyst.

Adapted from Wang and Yiu.¹⁴ with permission from the 2016 American Chemical Society.

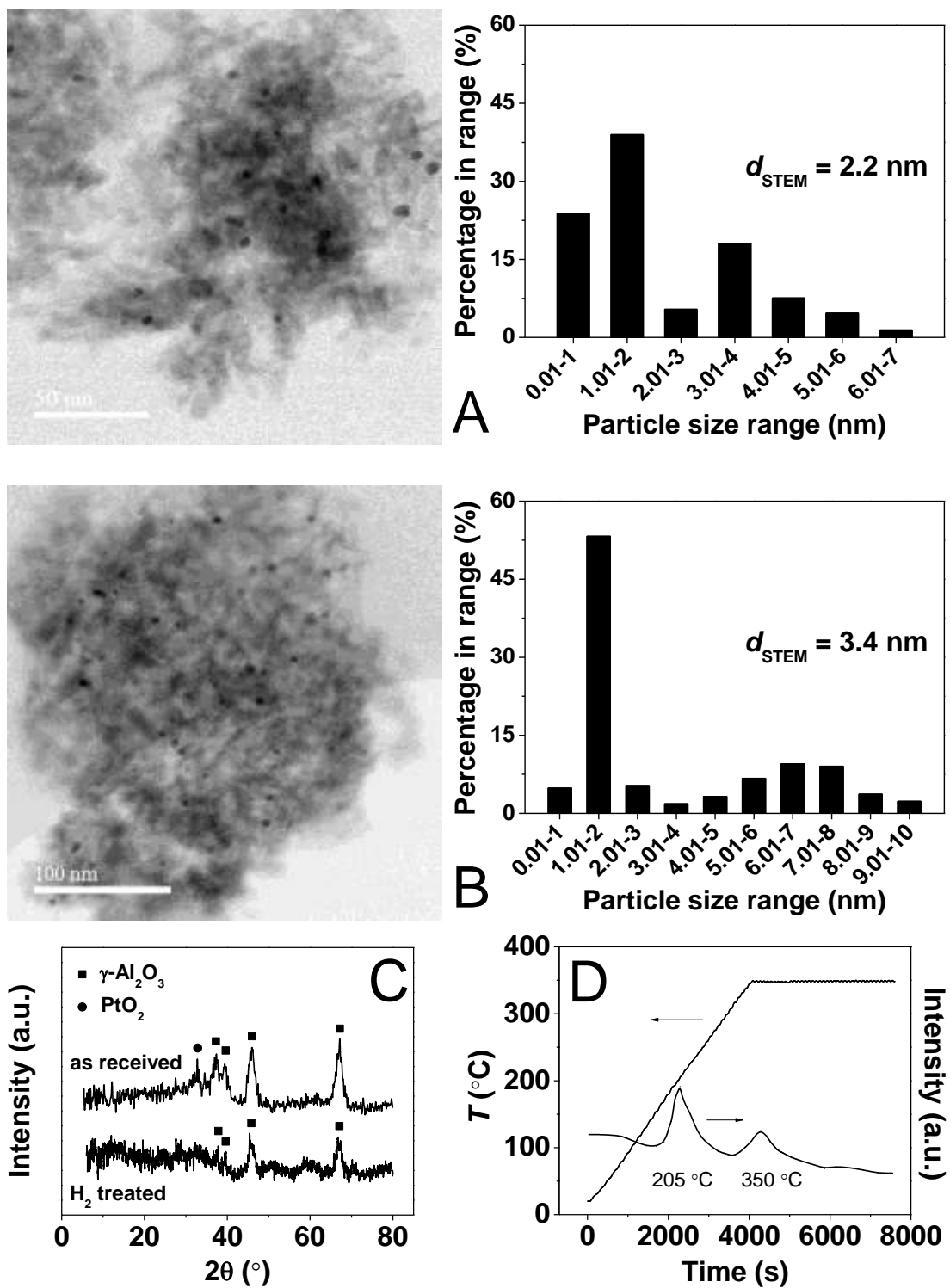


Figure 17. Characterization of Pt/Al₂O₃ (1 wt%)

- (A) Representative STEM image and Pt particle size distribution of the as received Pt/Al₂O₃.
 (B) Representative STEM image and Pt particle size distribution of the H₂ treated Pt/Al₂O₃.
 (C) XRD patterns for the as received and H₂ treated Pt/Al₂O₃.
 (D) TPR profile of the as received Pt/Al₂O₃.

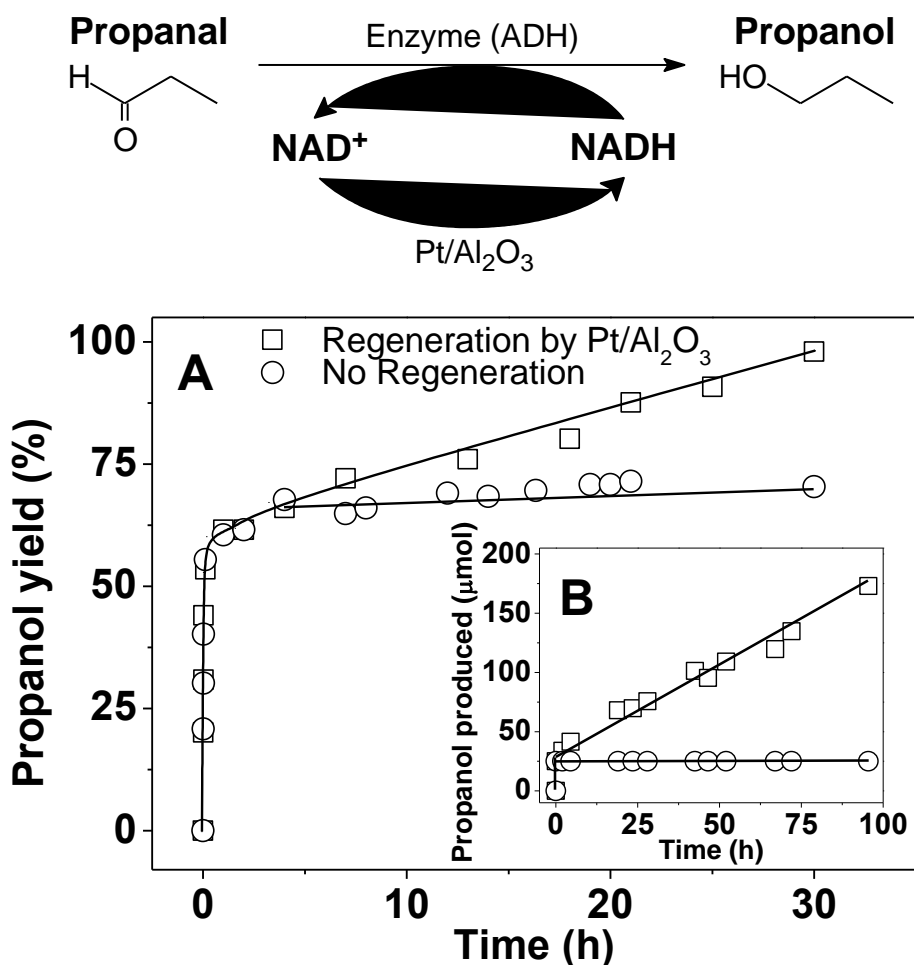


Figure 18. Enzymatic Reduction of Propanal to Propanol coupled with *in situ* NADH Regeneration by Pt/Al₂O₃

(A) Temporal propanol yield in batch enzymatic (ADH) reduction of propanal.

(B) Propanol production as a function of time in continuous enzymatic reduction of propanal.

Reaction conditions: $T = 20\text{ }^{\circ}\text{C}$, $P = 1\text{ atm}$ (H_2 flow = $30\text{ cm}^3\text{ min}^{-1}$), $\text{pH} = 8.8$ and 25 mg catalyst: (A) $[\text{NADH}]_0 = 7.0\text{ mM}$ and $[\text{propanal}]_0 = 10\text{ mM}$ and (B) initial $\text{NADH} = 25\text{ }\mu\text{mol}$ with propanal (2 mM) feed rate = $2.5\text{ cm}^3\text{ h}^{-1}$.

Adapted from Wang and Yiu.¹⁴ with permission from the 2016 American Chemical Society.